

Depositional Environment and Sequence Stratigraphy of the Oligocene-Miocene Deposits North and East of Dehdasht, Izeh Zone, Zagros Basin, Iran

F. Naseri-Karimvand¹, R. Moussavi-Harami^{*1}, A. Mahboubi¹,
A. Ghabeishavi², R. Shabafrooz²

¹ Department of Geology, Faculty of Science, International Campus, Ferdowsi University of Mashhad, Mashhad, Islamic Republic of Iran

² National Iranian South Oil Company (NISOC), Ahwaz, Islamic Republic of Iran

Received: 16 August 2017 / Revised: 12 November 2017 / Accepted: 12 February 2018

Abstract

In this study, four well-exposed outcrops of the Asmari Fm in the southeastern part of the Izeh Zone of the Zagros Mountains were measured and sampled. In this region, the Asmari Fm is Oligocene to Early Miocene in age as determined by large benthic foraminifera. Based on depositional geometries, biogenic contents and lateral and vertical variations of facies, three depositional models are proposed to illustrate the evolution of the Asmari carbonate platform. During the Chattian, large benthic foraminifera and coral-coralline red algae were dominant, while through the Early Miocene time interval (Aquitani an-Burdigalian), non-skeletal components along with porcelaneous foraminifera were the most conspicuous elements. These deposits formed a carbonate ramp in the Chattian and a low angle carbonate-ramp during the Early Miocene. Five major 3rd-order depositional sequences have been identified based on stratal stacking patterns and facies relationships. These depositional sequences show systematic progradations from SE to NW into and over the basinal Pabdeh Fm during Oligo-Miocene times.

Keywords: Asmari Fm, Zagros Mountains, Oligocene-Miocene, sequence stratigraphy.

Introduction

The Asmari Fm was deposited in the central segment of the Tethyan seaway in the Zagros Basin [1-3]. Extensive studies on the Oligo-Miocene Asmari Fm have been carried out since the 1960s [4-16]. These studies provide the basic information on the regional bio-and lithostratigraphy of the formation. More recently, detailed sedimentological, lithostratigraphic and biostratigraphic studies of the formation have been

carried out, with special attention to its depositional geometries and structures [1-3]. This paper presents a comprehensive sedimentological study of the Asmari Fm, adding details to the studies of Shabafrooz et al. [2 and 3] in order to have a better understanding of this stratigraphic interval in the adjacent oilfield areas. Therefore, the aims of this study are: (1) to describe facies and their distribution throughout the Oligocene-Miocene carbonate platforms and (2) to propose a sedimentological model for the Oligo-Miocene shallow-

* Corresponding author: Tel: +989151100937; Fax: +985138797572; Email: moussavi@um.ac.ir

water platforms.

Geological setting

The Zagros Orogeny is a well-known active, doubly-vergent and asymmetric mountain chain [17]. It is dominated by NW-SE oriented folds and thrusts, which swing into a NE trending towards the Strait of Hormuz (Fig. 1A). The mountain belt is divided into imbricated

and simply folded segments by the High Zagros and Mountain Front fault zones [18] (Fig. 1B). The Zagros Basin is subdivided into a number of zones (Lurestan, Izeh, Dezful embayment, Fars, High Zagros) [19, 20], and the study area is situated in the southeastern part of the Izeh Zone (Figs. 1B, C, 2).

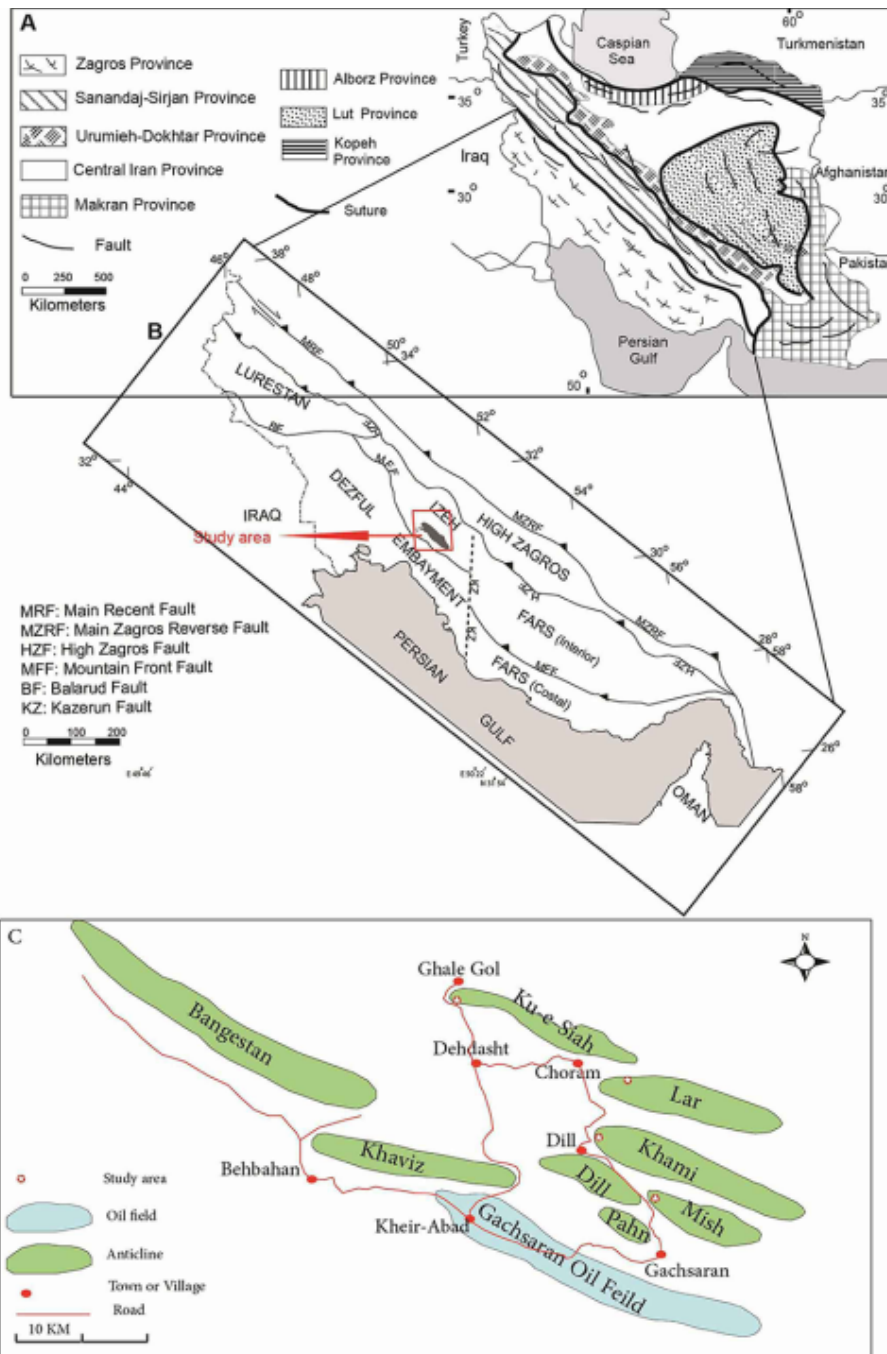


Figure 1. A) Structural map of the Zagros Mountain. B) Location of the study area in the Izeh Zone. C) Geographic map of the studied localities

Material and Methods

Four well-exposed outcrops (southern flank of the Mish anticline: thickness 440 m (Ganaveh); western plunge of the Khami anticline: thickness 248 m (Siang); northwestern flank of the Lar anticline: thickness 197 m (Arand), and western plunge of the Ku-e-Siah anticline: thickness 222 m (Dehdasht) were measured (Fig. 2), logged and sampled (sample density: 1–2/m). Close- and wide-view photo-mosaics were taken in order to analyze depositional geometries. More than 500 thin-

sections have been prepared for the identification of index fossils and facies textures. Also, the microfacies were classified based on the components and vertical changes [21-23]. The abundance of components for the quantitative description of the microfacies was defined as scarce (<5%), rare (5-10%), common (10-25%) and abundant (>25%). The sequence stratigraphy was analyzed with particular attention to discontinuity surfaces and depositional geometries along with the variation of stratal stacking patterns observed in the field.

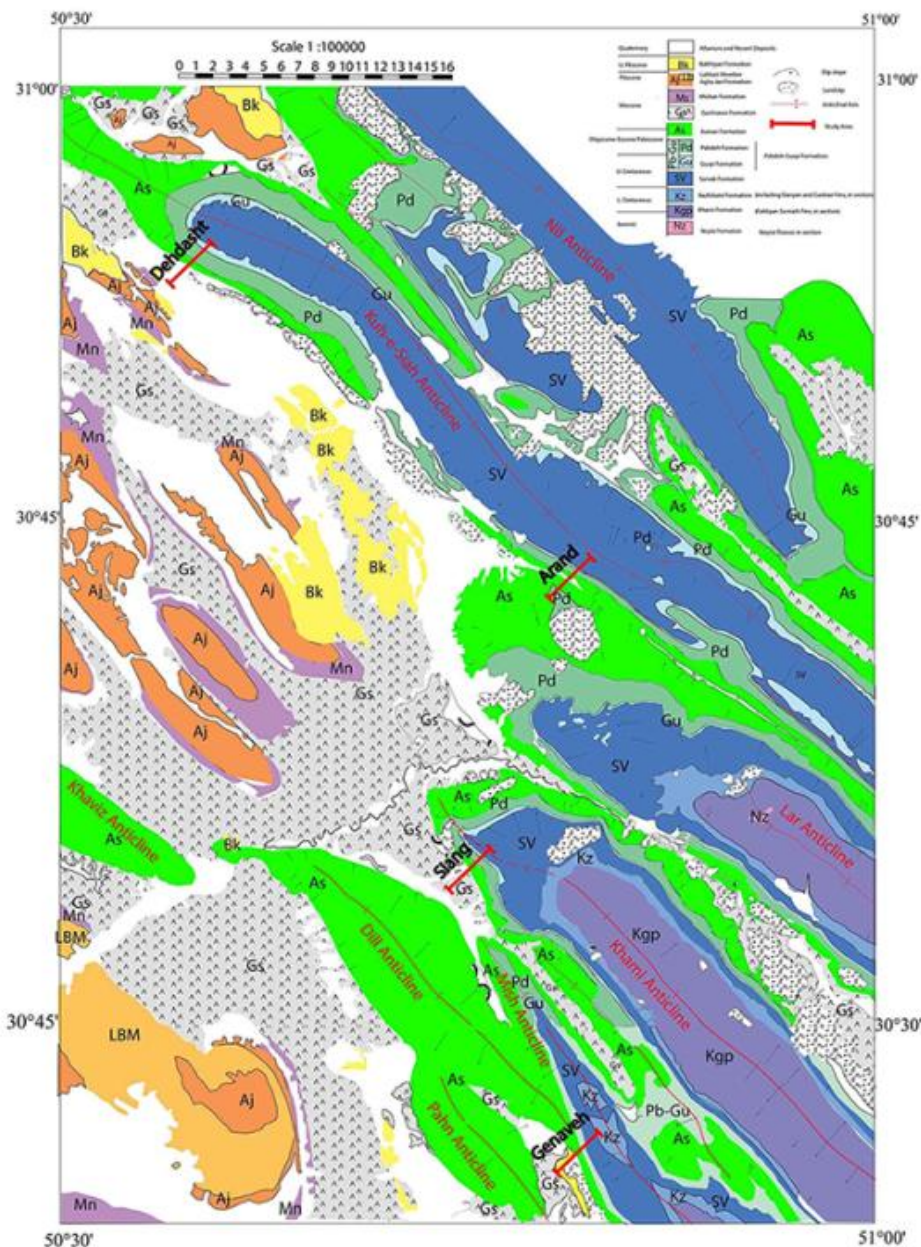


Figure 2. Geological map of the study area; Mish area (Ganaveh section), Khami (Siang section), Lar (Arand section), and Ku-e-Siah (Dehdasht section)

Results

Stratigraphy

The Asmari Fm is well exposed in Lurestan, Izeh, Fars (coastal and interior), and High Zagros zones [6]. The Oligo-Miocene deposits of the Asmari Fm have a

large variation in lithologies including sandstone, marl, carbonate and anhydrite with diachronous formation boundaries across these different zones. In the Izeh zone, the lower boundary of the Asmari Fm is in contact with the Pabdeh Fm, which is Paleocene-Oligocene in age [3], but in central Lurestan this formation overlies

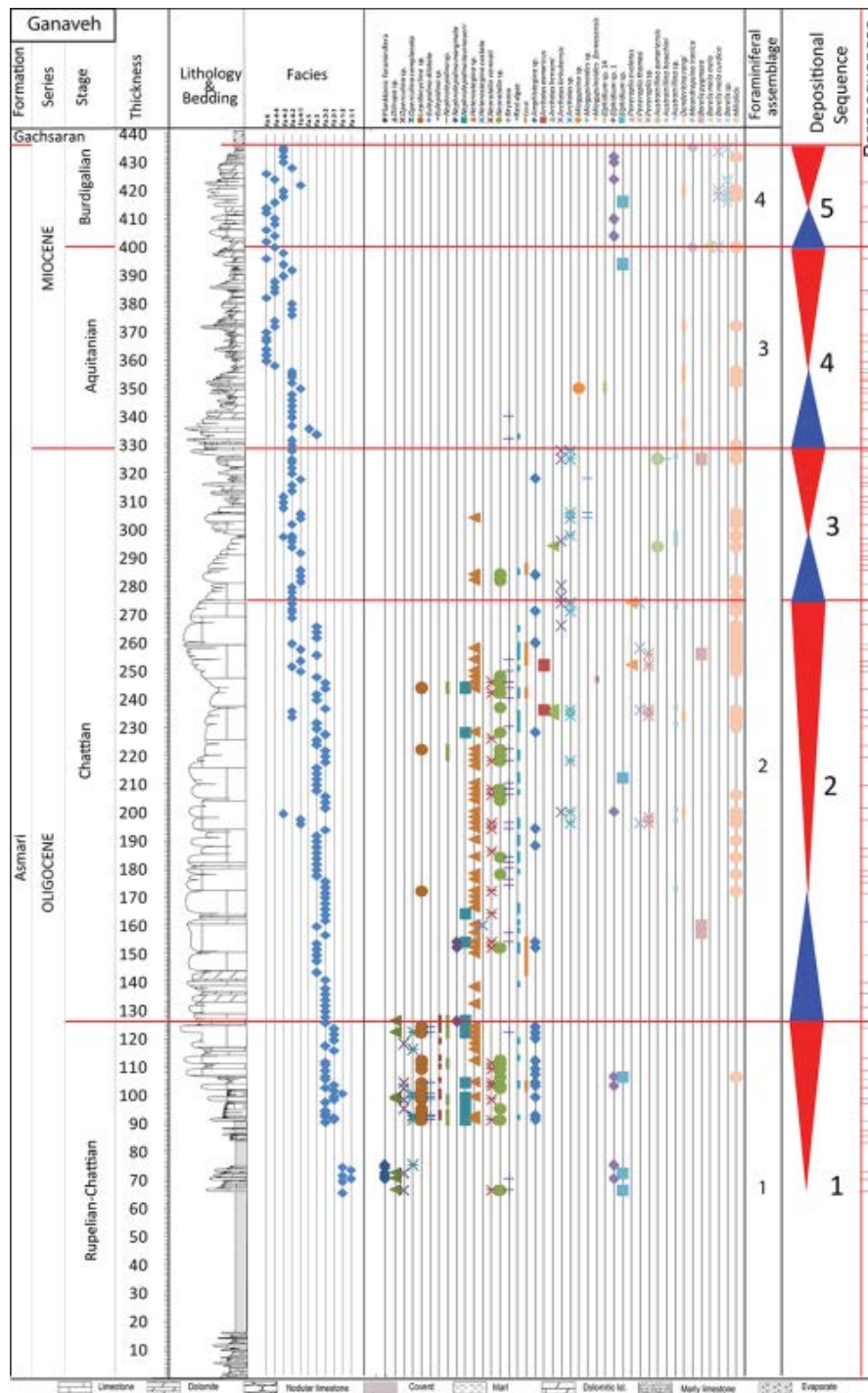


Figure 3. Litho and biostratigraphic column, vertical facies distribution and sequence stratigraphic characteristics of the Ganaveh section

the Late Eocene Shahbazan Formation [1] and in the Interior Fars it shows a paraconformable contact with the Jahrum Formation (Eocene) [5, 6, 24].

The Asmari Fm in the Izeh zone is covered by anhydrites of the Lower Miocene Gachsaran Formation [1, 3, 11], while in the Interior Fars it is covered by the Lower Miocene Razak Formation and the Eocene

Jahrum Formation [3, 14]. The base of the Asmari Fm is Lower Oligocene (Rupelian) in some areas and younger (Chattian) in other parts; while the top has different stratigraphic age ranging from Late Chattian to Early Miocene (Aquitanian - Burdigalian) [1-3, 8, 9, 11]. In the Fars zone, the Asmari Fm is Rupelian to Chattian in age [5, 14, 25], whereas in Izeh and the Dezful

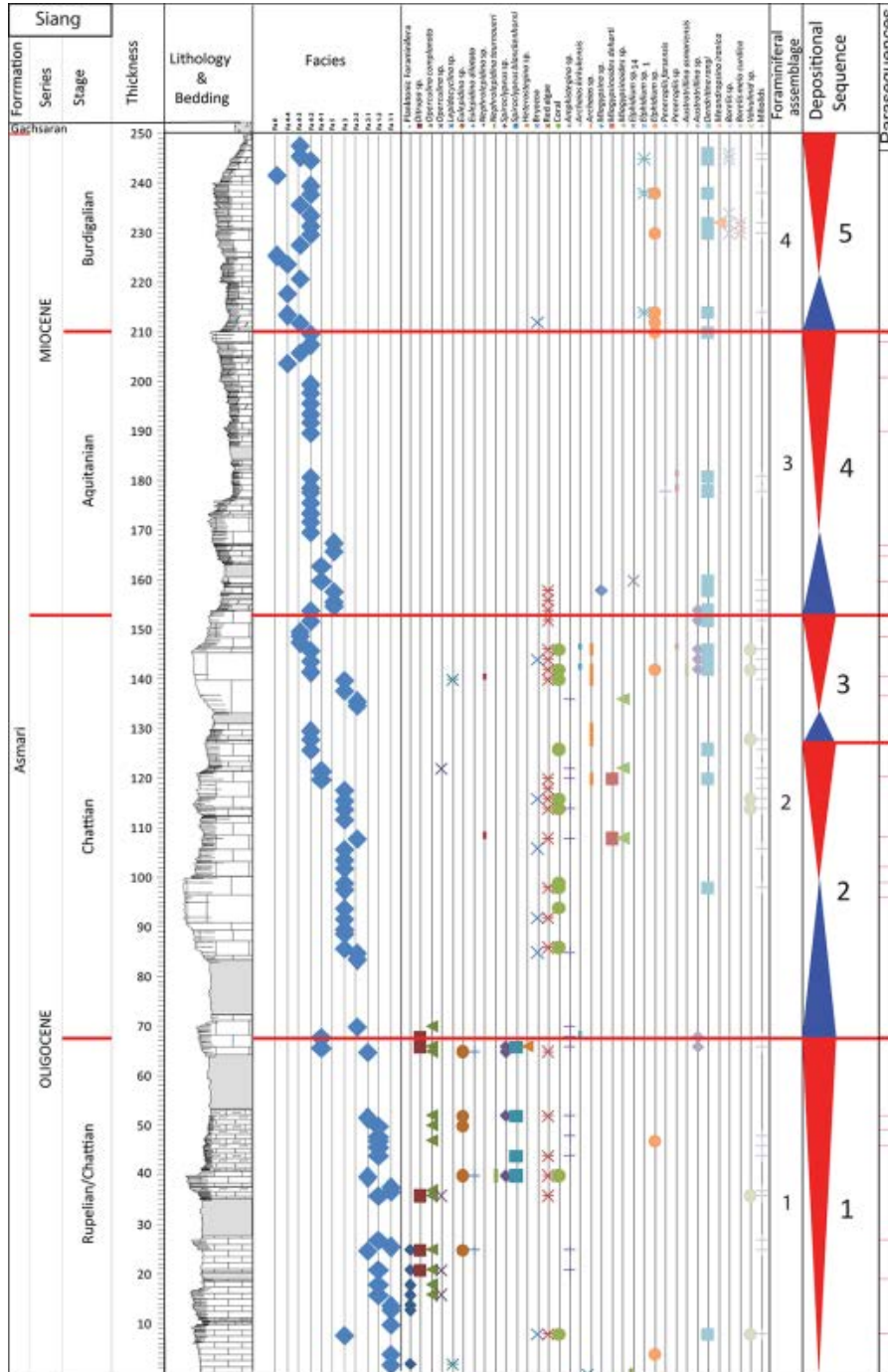


Figure 4. Litho and biostratigraphic column, vertical facies distribution and sequence stratigraphic characteristics of the Siang section. Legend as in Figure 3

embayment, the age of the formation is Rupelian to Early Burdigalian [1, 2, 11]. In the Lurestan Zone, the Asmari Fm is Chattian to Burdigalian in age [8]. In the study area, the Asmari Fm is composed of carbonate and overlies marls of the Pabdeh Fm.

Ganaveh section

The Ganaveh section is located at the Mish anticline (Figs. 1c, 2) and is the most proximal section in the study area. The Asmari Fm in this section is carbonate-dominated, reaching a total thickness of 440 m (Fig. 3), and overlies basinal marl of the Pabdeh Fm. The lower part of the interval in this section (from 0-126m) consists of an alternation of medium-bedded limestone (rich in LBF; mainly *Eulepidina*, *Operculina*, *Heterostegina*, etc.) and marl (rich in planktonic foraminifera), considered as a transitional zone between the Pabdeh and Asmari Fms, with a progressive decrease of fine-grained sediments up-section. This is followed by hundred meters of a massive-bedded limestone interval (from 120 to 275 m) which is characterized by large-scale coral-buildup. From 275–440 m, the section is characterized very extensive, tabular carbonate beds, mostly made of muddy facies rich in porcelaneous foraminifera associated with coral and coralline algae debris. The top is covered by the poorly preserved anhydrite beds of the evaporitic Gachsaran Formation (Fig. 3).

Siang section

The Siang outcrop is situated at the southern flank of the Khami anticline (Figs. 1c, 2), ~15 km aerial distance from the Ganaveh section. The Asmari Fm in this area is also carbonate-dominated and ranges a total thickness of 250 m (Fig. 4). In this area, the lower part of the Asmari Fm (0–68 m) consists of medium-bedded marly limestone with interbedded green marl rich in planktonic foraminifera and reworked fragments of LBF. The succession shows the upward transition from basinal marls of the Pabdeh Fm to carbonates of the Asmari Fm. This is followed by thick- to medium-bedded limestones (68-154 m), rich in porcelaneous benthic foraminifera, red algal fragments and corals with mostly packstone to boundstone texture.

The upper part of the Asmari Fm (154-255) at this locality consists of hundred meters of dolomitized limestone with locally nodular bedding, whereas elsewhere they are broadly bioturbated and brecciated. This succession contains a miscellaneous fauna including miliolids, *Dendritina*, *Borelis*, small rotaliids, discorbids, bryozoans and echinoid debris. The upper contact of the formation is marked by the Gachsaran Fm (Fig. 4).

Arand Section

The Arand section is situated at the northern flank of the Lar anticline (Figs. 1c, 2) an aerial distance of ~18 km from the Siang section. The Asmari Fm here is carbonate-dominated with a total thickness of 197 m (Fig. 5). The lower part (0-62 m) consists of meter-thick, marly limestone. This unit is followed by thin- to medium-bedded, highly dolomitized limestones (62-112 m) which are light grey to creamy in color. Among foraminifers, porcellaneous taxa are the most conspicuous, including both small and large forms.

The upper part of the Asmari Fm (112 -197 m) is composed of a thinning-upward succession of dolomitized lime mudstone with very rare miliolids, ostracod and ooids. Thick anhydrite beds (Gachsaran Formation) mark the top of the Asmari Fm (Fig. 5)

Dehdasht Section

The Dehdasht section is located at the southern flank of the Kuh-e Siah anticline (Figs. 1c, 2). It is about 222 m thick (Fig. 6); its aerial distance to the Arand section is about 26 km. The thick lower massive bedded limestones of the Asmari Fm in the Arand, Siang and Ganaveh sections pinch out into the Pabdeh Fm toward the Dehdasht section. At this locality, an alternation of medium-bedded marly limestones and marl (0- about 44 m), rich in planktonic foraminifera and fragments of LBF represent the initial deposits of the Asmari Fm overlying the basinal marl of the Pabdeh Fm.

There follows a thick succession (44-222 m) of relatively thin (1–2-m-thick), tabular carbonate beds alternating with creamy dolomite and highly dolomitized limestone beds. This interval is characterized by lagoonal facies, rich in porcelaneous foraminifera together with coralline algae debris. Furthermore, intercalations of ooids and *Favreina* grainstone/packstone are very common here. At this locality, the top of the Asmari Fm is in contact with the Gachsaran Formation (Fig. 6).

Biostratigraphy

Biostratigraphic zonation of the Asmari Fm was first introduced by Wynd [25], and later revised by Adams and Bourgeois [7]. Recently, Ehrenberg et al. [11] and Van Buchem et al. [1] recognized a further accurate age control of the Asmari Fm. In the present paper, LBF are used to date the Asmari Fm using these zonations. It has also been compared with the global Oligocene/Miocene zonation of Cahuzac and Poignant [26]. As a result, based on the micropaleontological analysis of the larger benthic foraminifera and their distribution, four assemblage zones have been identified (Table 1).

(1) The occurrence of *Lepidocyclina* (*Eulepidina*)

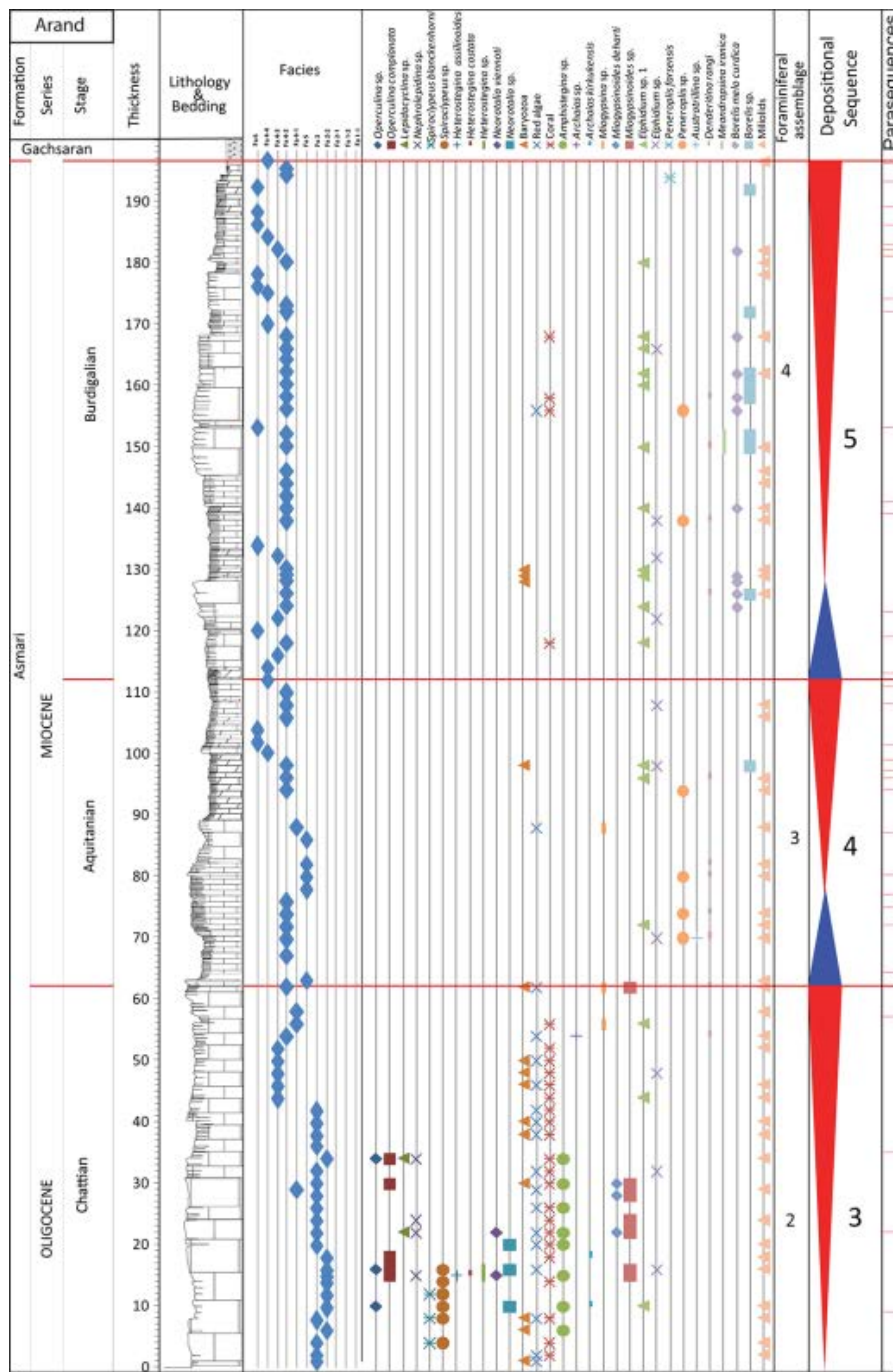


Figure 5. Litho and biostratigraphic column, vertical facies distribution and sequence stratigraphic characteristics of the Arand section. Legend as in Figure 3

dilatata and the absence of *Nummulites* in the lower parts of the Asmari Fm in the Ganaveh (Fig. 3), Siang (Fig. 4) and Arand (Fig. 5) sections indicate a Rupelian/Chattian age corresponding to the “*Lepidocyclina – Operculina - Ditrupa*” Assemblage Zone (Assemblage C; Table 1) of Van Buchem et al. [1] and the SBZ 22 of Cahuzac and Poignant [26]. This

biozone disappears towards the Dehdasht section as the carbonate of the Asmari Fm laterally changes to the basal marl of the Pabdeh Fm.

(2) The occurrence of *Archaias* (*A. kirkukensis* and *A. hensoni*) as well as the presence of *Miogypsinoides complanatus* in the middle part of the Asmari Fm in the Ganaveh (Fig. 3), Siang (Fig. 4), Arand (Fig. 5) and

correspond to the *Miogypsina - Elphidium* sp. 14 - *Peneroplis farsenensis*” Assemblage Zone (Assemblage E; Table 1) of Van Buchem et al. [1] and the SBZ 24 of Cahuzac and Poignant [26] and is attributed to the Aquitanian.

The Aquitanian does not exhibit any significant thickness variations throughout the study area and has a limited diversity of components such as *Favreina asmarica*, *Miogypsina*, few miliolids, *Dendritina*, and ooids. The decapod coprolite *Favreina asmarica* represents hypersaline conditions during the Aquitanian [1].

(4) The upper parts of the Asmari Fm at all sections contain *Borelis melo curdica* corresponding to the *Borelis melo curdica - B. melo melo*” Assemblage Zone (Assemblage G; Table 1) of Van Buchem et al. [1] and the SBZ 25 of Cahuzac and Poignant [26] which indicate a Burdigalian age.

Facies analysis

The microscopic and macroscopic study is resulted the recognition of six facies associations (FA.1-6). These FA consist of 11 sub-Facies (Sub-F) along the depositional profile (Table 2), from basin to shoreline.

Table 1. Biozonation of the Asmari Fm in the study area

Stage	No Van Buchem et al. (2016)	Assemblage zone	Ma.	Foraminiferal Assemblage	Location	SBZ Cahuzac and Poignant (1997)
Burdigalian	G	<i>Borelis melo curdica</i> - <i>Borelis melo melo</i> <i>Dendritina rangi</i> + <i>Meandropsina</i> spp. + <i>Spirulina</i> spp. + <i>polymorphinids</i> + <i>Discorbis</i> sp. + Small peneroplids + <i>Peneroplis evolutus</i> + miliolids + Echinoid debris	18.2 to 20.2	4	Ganaveh, Siang, Arand, Dehdasht	SBZ 25
Aquitanian	F	Indeterminate Zone Very poor of fossils + Unidentified Miliolids + <i>Dendritina rangi</i>	20.2 to 22.2	-	-	-
Aquitanian	E	<i>Miogypsina - Elphidium</i> sp. 14 - <i>Peneroplis farsenensis</i> <i>Miogypsina</i> spp. + <i>Elphidium</i> sp. 14 + <i>Peneroplis farsenensis</i> + <i>Favreina asmarica</i>	20.2 to 23	3	Ganaveh, Siang, Arand, Dehdasht	SBZ 24
Chattian	D	<i>Archaias asmaricus / hensoni</i> - <i>Miogypsinoides complanatus</i> <i>Archaias hensoni</i> + <i>Archaias asmaricus</i> + <i>Miogypsinoides complanatus</i> + <i>Spirochypers blanchenhorni</i>	23 to 28.2	2	Ganaveh, Siang, Arand, Dehdasht	SBZ 23
Rupelian Into Chattian	C	<i>Lepidocyclina - Operculina - Ditrupa</i> <i>Eulepidina dilatata</i> + <i>Heterostegina</i> spp. + <i>Rotalia viemoti</i> + <i>Haplophragmium slingeri</i> + <i>Planorbulina</i> spp. + <i>Algae</i>	23 to 32.3	1	Ganaveh, Siang, Arand	SBZ 22
Rupelian	B	<i>Nammulites vascus</i> - <i>Nammulites fichteli</i> <i>Operculina complanata</i> + <i>Heterostegina</i> spp. + <i>Rotalia viemoti</i> + <i>Eulepidina dilatata</i> + <i>Eulepidina elephantina</i> + <i>Archaias operculiniformis</i> + <i>Subterranophyllum thomasi</i> + <i>Haplophragmium slingeri</i> + <i>Ditrupa</i> sp.	28.2 to 33.4	-	-	-
Eocene to E. Oligocene	A	<i>Globigerina</i> spp. - <i>Turborotalia cerroazulensis</i> - <i>Hantkenina</i> <i>Globigerina</i> spp. - <i>Turborotalia cerroazulensis</i> - <i>Hantkenina</i> sp.	30 to 33.5	-	-	-

Table 2. Summary of the facies and facies associations in the Asmari Fm of the study area

Facies / facies association	Components	Sorting	Depositional environment	Locations				Age			
				Ganaveh	Siang	Arand	Dehdasht	Rupelian/Chattian	Chattian	Miocene	
FA.5 II	Mudstone/siltstone/mudstone	Rare angular-sub angular sand.	Poor	Proximal inner-ramp	✓	✓	✓	✓			✓
FA.5 III	Favreina ooid-grainstone/packstone	Bioclast of bivalve, gastropods and echinoids. Spheroidal ooids, micritic ooids, forams. Rare <i>Miogypsina</i> and miliolids.	Good to moderate	High energy shoal	✓	✓	✓	✓			✓
Facies association I	Subfacies 4-4: Low diversity imperforate foraminiferal wackestone/packstone	Small miliolids and <i>Dendritina</i> . Rare fragments of echinoids and bivalves.	Poor	Lagoon	✓	✓	✓	✓			✓
	Subfacies 4-3: Small perforate foraminiferal-echinoid wackestone/packstone	Abundant fragments of echinoids, bivalve and bryozoa. Abundant eophytic foraminifera (<i>Spirulina</i> , small rotalia and small miliolids). Rare <i>Ammonia</i> , <i>Foraminifera</i> and ostracods.	Poor	Lagoon	✓	✓	✓	✓			✓
	Subfacies 4-2: High diversity imperforate foraminiferal packstone/grainstone	Abundant symbiont-bearing porositaneous foraminifera (<i>Archaias</i> , <i>Borelis</i> , <i>Peneroplis</i> , <i>Austrorotalia</i> , <i>Dendritina</i>) and small miliolids. Rare crinoids and nodules of articulated red algae and fragments of corals. Rare small perforate foraminifera (<i>Spirulina</i> and rotalia) and foraminifera.	moderate	Medio of inner-ramp (Semi-protected lagoon)	✓	✓	✓	✓			✓
	Subfacies 4-1: Perforate/imperforate foraminiferal wackestone/packstone to grainstone	Frequent miliolids and symbiont-bearing porositaneous foraminifera (<i>Archaias</i> , <i>Peneroplis</i>). Large rotalia includes: <i>Amphistegina</i> , <i>Neorotalia</i> , <i>Operculina</i> , <i>Miogypsinoides</i> . Fragments of coral and coralline red algae. Fragments of echinoids, bivalves and gastropods.	Moderate	Distal inner-ramp (Open lagoon)	✓	✓	✓	✓			✓
FA.3 I	Coralline red algal coral rudstone/siltstone	Rhodoliths, abundant crust of non-articulated red algae. Patch and scattered coral, coral encrusted by red algae, bryozoa fragments, Echinoids and small miliolids.	Poor	Proximal mid-ramp	✓	✓	✓	✓			✓
Facies association II	Subfacies 2-2: Mammulid-Neorotalia siltstone/packstone to grainstone	Intact <i>Neorotalia</i> (<i>Neorotalia viemoti</i>) and well-preserved <i>Amphistegina</i> , abundant <i>Nammulites</i> (<i>Heterostegina</i> sp., <i>Operculina</i> sp.). Fragments of red algae and echinoids. Low amount of fragments of coral, bivalve and bryozoa.	Poor	Medio of mid-ramp	✓	✓	✓	✓			✓
	Subfacies 2-1: Mammulid lepidocyclid foratone/rudstone	Intact LBF such as <i>Lepidocyclina</i> (<i>Eulepidina aliana</i> and <i>Lepidocyclina</i> sp.), <i>Nammulites</i> (<i>Operculina</i> complex, <i>Spirochypers blanchenhorni</i> and <i>Heterostegina</i> sp.) Broken test of LBF. Accessory foraminifera includes <i>Neorotalia</i> and <i>Amphistegina</i> . Bryozoa and red algae are rare.	Poor	Distal mid-ramp	✓	✓	✓	✓			✓
Facies association III	Subfacies 1-2: Mammulid planifera foraminiferal wackestone/packstone	Bioclast, <i>Globigerina</i> , <i>Operculina complanata</i> , <i>Neorotalia</i> sp., <i>Ditrupa</i> sp., <i>Lepidocyclina</i> sp., echinoids and very rare miliolids, corals and red algae.	Poor	Toe of slope (Outer ramp?)	✓	✓	✓	✓			✓
	Subfacies 1-1: Planifera foraminiferal wackestone/packstone	Bioclast, <i>Globigerina</i> , <i>Ditrupa</i> sp., Echinoids, bryozoa and small benthic foraminifera such as <i>Elphidium</i>	Poor	Outer ramp	✓	✓	✓	✓			✓

A more detailed analysis of these facies associations is tabulated in Table 2 and their summary narrations and in-detail environmental interpretations were discussed in the following.

Facies association 1: Planktonic foraminifera wackestone/packstone

This FA basically consists of thin to medium-bedded limestone (mudstone /wackestone to packstone in texture) with interbedded green marl. Two subfacies are notable: planktonic foraminifera wackestone/-packstone (Subfacies 1-1) and bioclast planktonic foraminifera, nummulitid wackestone/-packstone (Subfacies 1-2).

Subfacies 1-1: Planktonic foraminiferal wackestone/-packstone

The main constituents of this facies are planktonic foraminifera (globigerinids and globorotaliids), *Ditrupa* and fine fragments of hyaline foraminifera tests with mainly mud-dominated textures (wackestone to packstone). Fragments of echinoids, bryozoans and bivalves are also present (Fig. 7A). This facies occurs in thin- to medium-bedded limestone and marl of the transition zone between the Pabdeh and Asmari Fms. The fine-grained nature of the sediments along with the presence of planktonic foraminifera and the muddy texture suggest that this facies has been deposited in a

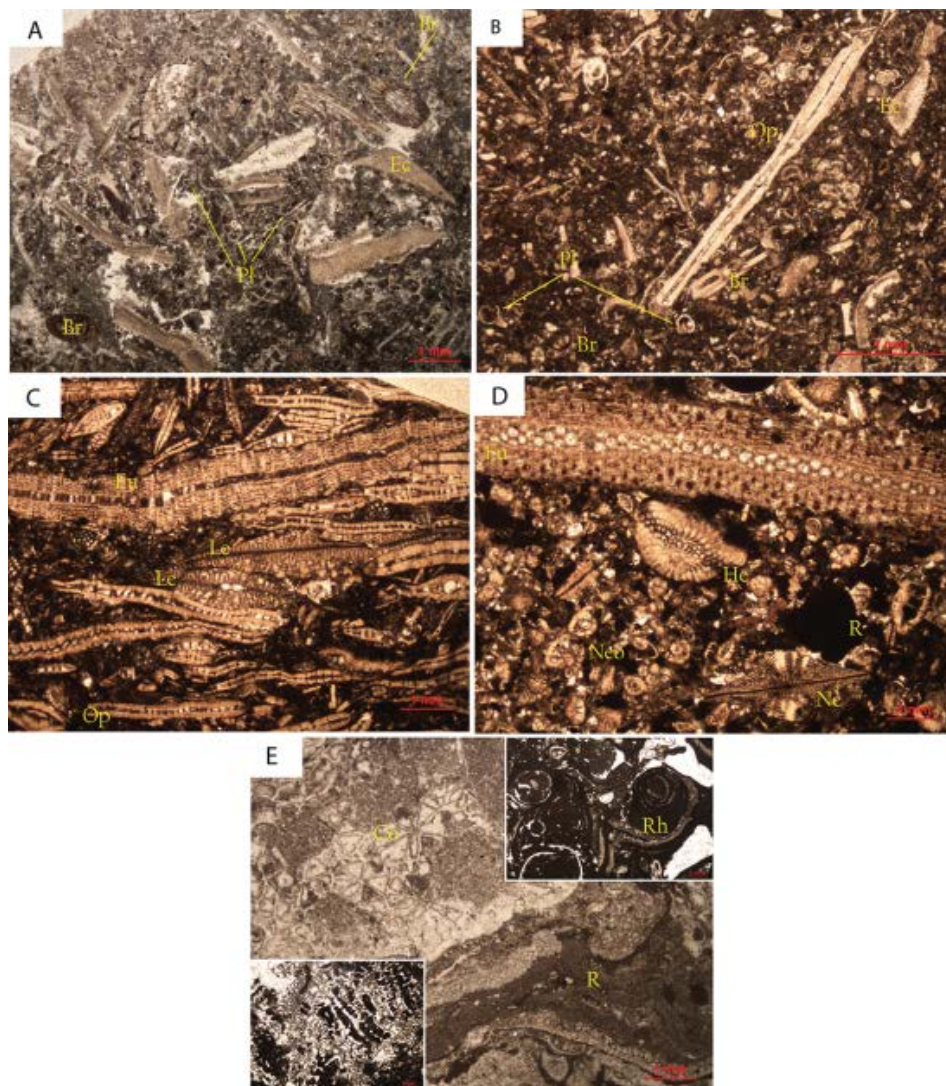


Figure 7. A) Planktonic foraminiferal bio-wackestone/-packstone (Pl: Planktonic foraminifera, Ec: echinoid, Br: bryozoan). B) Nummulitid-planktonic foraminiferal bio-wackestone/packstone (Pl: planktonic foraminifera, Op: *Operculina*, Ec: echinoid, br: bryozoan). C) Nummulitidae-Lepidocyclinidae bio-floatstone/-rudstone (Eu: *Eulepidina*, Le: *Lepidocyclina*, Op: *Operculina*). D) Lepidocyclinid- *Neorotalia* bio-rudstone/-packstone to -grainstone (Eu: *Eulepidina*, He: *Heterostegina*, Neo: *Neorotalia*, Ne: *Nephrolepidina*, R: red algae). E) Coralline red algae-coral rudstone/floatstone (Rh: rhodolith, Co: coral, R: red algae).

low energy setting, probably in the outer ramp/basin [2, 22, 27-29].

Subfacies 1-2: Nummulitid planktonic foraminiferal wackestone/-packstone

This facies consists of dark grey to brown limestone (interbedded with facies 1), occasionally argillaceous, bioturbated wackestones or packstones (Fig. 7B), characterized by the occurrence of large benthic and planktonic foraminifera (globigerinids and globorotaliids). The larger benthic foraminifera are Nummulitidae (mainly *Operculina*) and Lepidocyclinidae such as *Eulepidina* that are often abraded and fragmented. Other bioclastic components in this facies are fragments of *Ditrupa*, echinoderms and bryozoans (Fig. 7B). The abundance of marine biota (perforated larger benthic foraminifera) along with planktonic foraminifera indicates that this facies probably was deposited in the transition zone between basin (outer ramp?) and platform slope [2, 8, 30-32].

Facies association 2: Nummulitid-lepidocyclinid rudstone-packstone

This FA consists of metre-thick, marly limestone with planar bedding, including two subfacies: nummulitid-lepidocyclinid rudstone/floatstone (Subfacies 2-1) and *Neorotalia*-*Lepidocyclina*-coralline algae packstone (Subfacies 2-2).

Subfacies 2-1: Nummulitid lepidocyclinid floatstone/-rudstone

This facies forms beds with medium thickness and can be easily used as a marker for outcrop correlation. Large and flat (0.3–10 cm) perforate benthic foraminifera, typically lepidocyclinids and *Operculina* (Fig. 7C), are dominant biogenic components. Other genera include *Spiroclypeus*, *Heterostegina* and *Amphistegina*. All these biogenic components are well preserved. This facies is most dominant in the lower parts of the Asmari Fm and typically intercalated with Facies 1 or grades into Facies 2.

These features show that this facies has been deposited in a low-energy environment, below the fair-weather wave-base [33]. Deep-living foraminifera such as large and flat *Eulepidina*, *Nephrolepidina*, *Operculina*, *Heterostegina*, *Spiroclypeus* and fragments of echinoids resistant to mechanical abrasion suggest that sedimentation may have taken place in deeper parts of the oligophotic zone [34, 35].

Subfacies 2-2: Nummulitid-Neorotalia rudstone/-packstone to -grainstone

In this facies, thick and well-preserved *Neorotalia*

and *Amphistegina* are abundant in a packstone to grainstone texture. Other common components include Nummulitidae (mostly *Heterostegina* and *Operculina*) and *Miogypsinoides*. Red algae, echinoid fragments and a mixture of intact and broken tests of Lepidocyclinidae (*Eulepidina* and *Nephrolepidina*) are also present. Coral fragments are rare (Fig. 7D).

The thick *Neorotalia* and inflated *Amphistegina* tests may indicate mesophotic conditions [33, 36]. The presence of flat nummulitids and Lepidocyclinidae and non-articulated red algae are indicative of the oligophotic zone [33, 37, 38]. Co-occurrence of flat and inflated foraminifera may be related to reworking of shallow-water forms, but there is no evidence of transport-induced test abrasion or damage.

Facies association 3: Coralline red algal coral rudstone/floatstone

This facies is characterized by the thick to massive bedding limestone rich in corals and non-articulated coralline red algae. Coralline red algae are present as rhodoliths, crusts, and nodules. The components that are encrusted by coralline red algae are bryozoans, bivalves, gastropods, and foraminifera (Fig. 7E). The corals form patch reefs and build-ups (Fig. 8A-C) and locally corals are encrusted by coralline red algae.

The rhodolithic facies is indicative of moderate to low energy conditions that may have formed in oligophotic settings [39, 40]. The optimal conditions for coral growth existed below the sea grass meadow. They did not form wave-resistant rigid frameworks rising up to the sea level, but built small and discrete build-ups [33]. Where corals are encrusted by red algae, this can be evidence for meso-to oligophotic conditions.

Facies Association 4: Benthic foraminifera wackestone-grainstone

This facies association includes four subfacies: *Perforate/imperforate foraminiferal wackestone/-packstone to grainstone* (Subfacies 4-1), *High diversity imperforate foraminiferal packstone/-grainstone* (Subfacies 4-2), *Small perforate foraminiferal-echinoid wackestone/-packstone* (Subfacies 4-3), and *Low diversity imperforate foraminiferal wackestone /-packstone* (Subfacies 4-4).

Subfacies 4-1: Perforate/imperforate foraminiferal wackestone/-packstone to grainstone

The most common foraminifera in this facies are miliolids (*Triloculina*, *Quinqueloculina*, *Austrorillina* and *Pyrgo*) and symbiont-bearing forms (*Archaias*, *Peneroplis* and *Denderitina*). Additional forms are *Amphistegina*, *Neorotalia*, *Nephrolepidina*, nummulitids

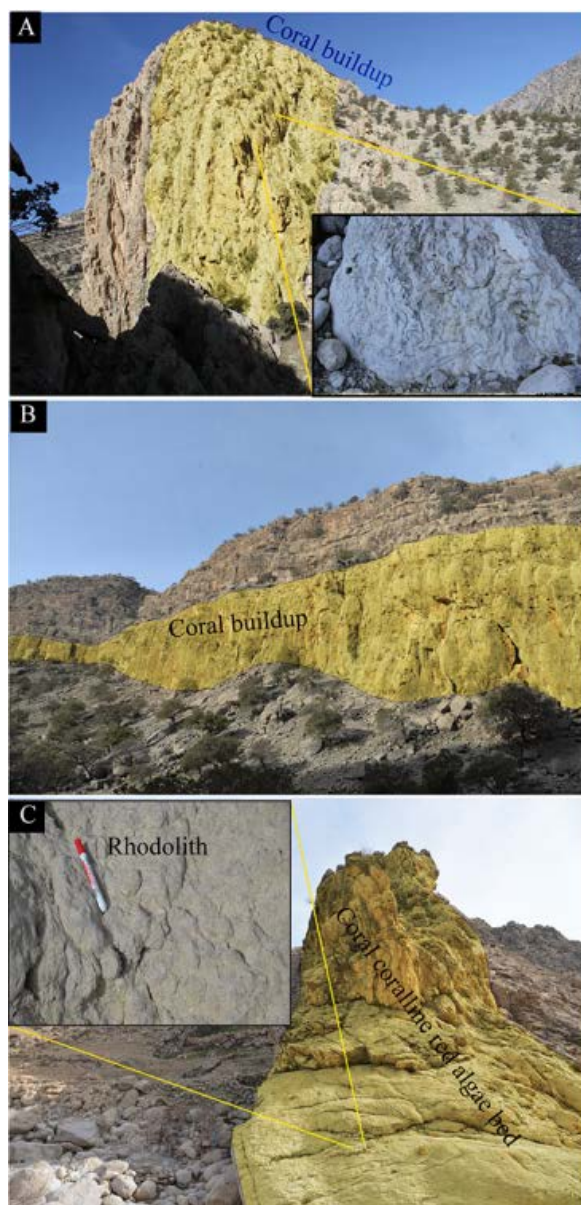


Figure 8. A) Distant and close-up view of the coral build-up in the Ganaveh section. B) Geometry of the coral build-up in the Arand section. C) Close-up view of coral coralline red algal bed and detail view of the rhodolith in the Dehdasht section.

(mostly *Operculina*, *Heterostegina*) and miogypsinids (*Miogypsinoides*, *Miogypsina*). Coralline red algal fragments and scattered corals also occur. Fragments of echinoderms and bivalves are the most common heterotrophic organisms (Fig. 9A).

Co-occurrence of large porcelaneous foraminifera, such as *Archaias*, *Peneroplis* and *Austrorillina* and hyaline forms, suggests a lagoon with free water circulation within the euphotic zone [34, 41, 42].

Subfacies 4-2: High diversity imperforate foraminiferal packstone/-grainstone

Abundant imperforate foraminifera include *Archaias*, *Austrorillina*, *Peneroplis*, *Borelis* and *Dendritina*. Miliolids are commonly found in this facies as are fragments of echinoderms, bivalves and bryozoans. Fragments of corals and coralline red algae are locally present. Small perforate foraminifera (*Elphidium*, rotaliids, *Reussella*, and *Discorbis*) are rare (Fig. 9B).

The presence of symbiont-bearing porcelaneous (*Archaias*, *Borelis*, *Peneroplis*) and epiphytic (*Discorbis*, *Elphidium*, *Planorbulina*) foraminifera is indicative of sea-grass meadow environments within the euphotic zone [37, 43, 44]. The scattered corals and branched free-living red algae may be related to deeper parts of the euphotic zone. Large porcelaneous foraminifera in grainstone texture along with abraded biogenic components reveal that the sediment formed in the agitated-wave zone of the lagoonal environment [45, 46].

Subfacies 4-3: Small perforate foraminiferal-echinoid wackestone/-packstone

Small benthic foraminifera (small rotaliids, *Elphidium*, *Discorbis*, miliolids) and echinoid fragments are common. Large porcelaneous foraminifera such as *Dendritina*, *Borelis* and *Quinqueloculina* are rare. Ostracods, *Reussella*, textulariids and *Ammonia* are very rare (Fig. 9 C). Depending on phytal substrate, large porcelaneous and epiphytic foraminifera indicate an expanded-sea grass environment within the euphotic zone [44, 47-50]. Thus, *Ammonia* and textulariids are low-oxygen tolerant foraminifera being able to live under dysoxic to anoxic conditions [49].

Subfacies 4-4: Low diversity imperforate foraminiferal wackestone/-packstone

The main texture of this facies is wackestone; it occurs less commonly in packstone with small miliolids and *Dendritina*. Other constituents include *Peneroplis*, *Discorbis*, textulariids and ostracods. Echinoids and bivalve debris are very rare (Fig. 9D). Due to the low diversity of imperforate foraminifera and its texture, this facies formed in low-energy, very shallow and hypersaline waters probably within a protected shelf lagoon [8, 38]. Today, euryhaline small miliolids live on flat bottoms in very shallow environments (upper part of the photic zone [32].

Facies Association 5: Favreina ooid-grainstone/packstone

This facies has a limited geographic distribution

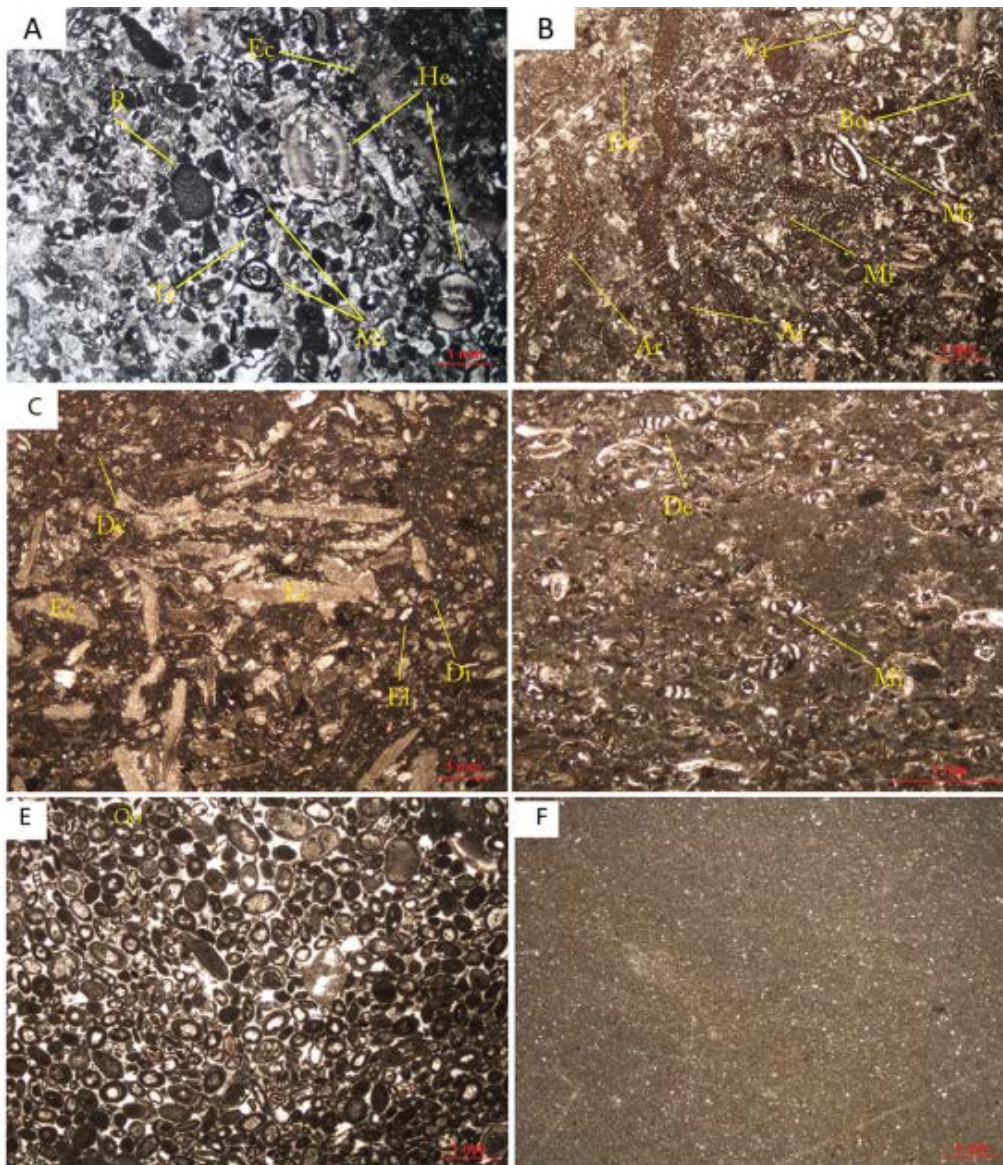


Figure 9. A) Perforate–imperforate foraminiferal bio-packstone/-wackestone to -grainstone (He: *Heterostegina*, Ec: echinoid, R: red algae, Te: textularids, Mi: miliolid). B) High-diversity imperforate foraminiferal bio-packstone/-wackestone (Ar: *Archaias*, Bo: *Borelis*, Va: valvulinid, Mi: miliolid, De: *Dendritina*). C) Small perforate foraminiferal–echinoid bio-wackestone/-packstone (Di: *Discorbis*, El: *Elphidium*, De: *Dendritina*, Ec: echinoid). D) Low-diversity imperforate foraminiferal bio-wackestone/-packstone. E) Ooid grainstone. F) Mudstone (Mi: miliolid, De: *Dendritina*).

(Dehdasht section), characterized by medium-bedded limestone, mainly composed of ooids, peloids and bioclasts with packstone to grainstone texture. The beds are decimetre- to metre-scale thick (up to 2 m) and locally contain cross-stratification. Two types of ooids, superficial with a thin cortical layer and micritic, have been identified. The nuclei of the ooids include small miliolids, bioclasts and intraclasts. Other common components are *Favreina*, bivalves, gastropods and echinoderms. *Miogypsina* and small benthic foraminifera (*Elphidium*, *Reussella*, and small rotaliids)

are rare (Fig. 9E). Well-sorted, grain-dominated textures and a variety of skeletal fragments in this facies show a high-energy ooid shoal under the influence of fair-weather waves and local tides [51, 52]. The *Favreina* grainstone along with ooids and bioclasts suggests that the high energy shoal formed under hypersaline conditions [22].

Facies Association 6: Mudstone/dolomitic mudstone

This facies is characterized by a mudstone texture with scattered fine quartz grains and very scarce

echinoid debris (Fig. 9F). Moreover, casts of evaporate minerals (gypsum crystals) are locally present. In some thin-sections, dolomite crystals are present. This facies occurs in thin- to medium-bedded dolostones, dolomitic limestones and pure limestones. This evidence indicates that deposition occurred in a hypersaline, very shallow and protected lagoon, probably towards the supratidal zone [2, 3, 8].

Depositional environments

The depositional models of the Asmari Fm (Fig. 10) were reconstructed based on tracing strata in the field and evaluations of photographs. These information were subsequently tied to the measured sections by using bedding geometries, relative position of facies belts, sedimentary structures and the dependence of some

skeletal components upon light penetration [53]. These characteristics indicate that in the study area the Asmari Fm represents a carbonate ramp in the Chattian and a very low-angle carbonate ramp during Early Miocene time. In the following, three depositional models are presented for the time slices Rupelian- Chattian, Aquitanian and Burdigalian (Fig. 10 A-C).

Rupelian-Chattian carbonate ramp system

The facies model presented for the Oligocene of the Asmari platform shows a depth gradient from the inner to mid and outer ramp, corresponding with distribution pattern of foraminifera and calcareous algae. During this time interval, the study area occupied the distal parts of the mid to outer ramp (Fig. 10A). That is, the Dehdasht and Arand sections were located in the outer ramp

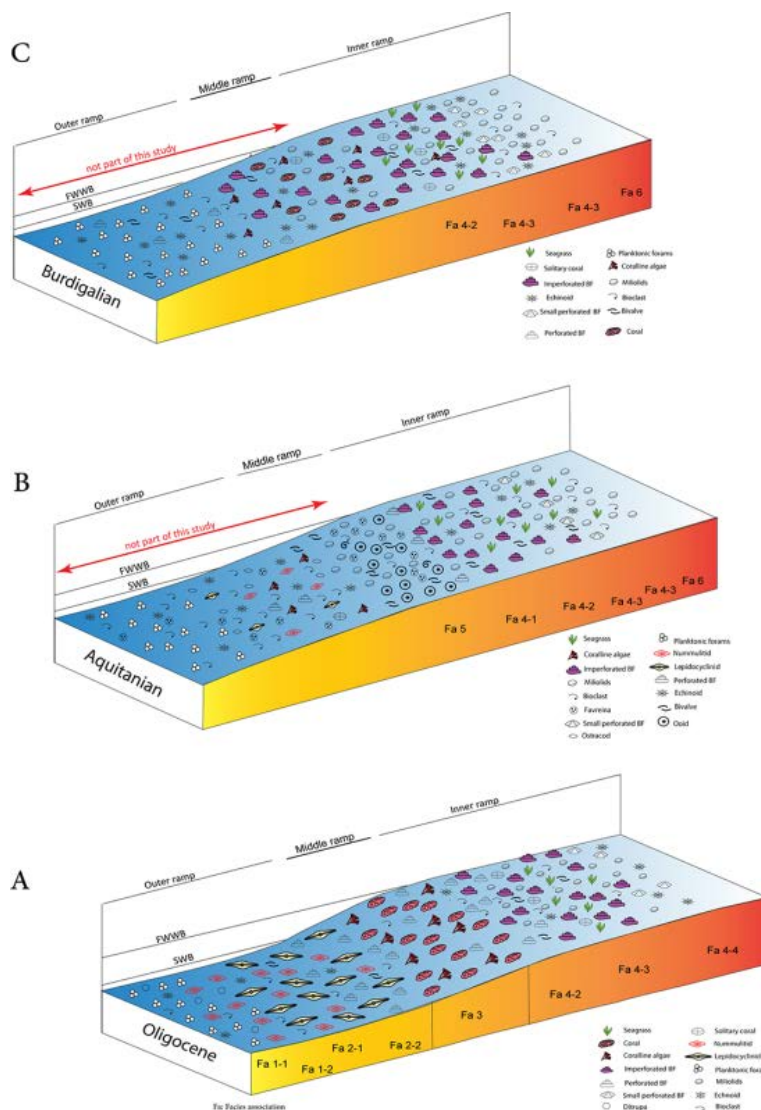


Figure 10. Schematic depositional models for the Asmari Fm during Oligocene (A), Aquitanian (B) and Burdigalian (C) times.

settings, while the Siang and Ganaveh sections were in the mid ramp settings of the carbonate platform. The inner parts of the carbonate platform were probably located further to the NE, outside the study area. The facies model presented here shows a depth gradient from (1) highly transparent and shallowest part of the ramp (inner ramp) characterized by facies association 4, (2) the shallow part of the middle ramp with facies association 2, to (3) deeper middle ramp to shallower part of the outer ramp settings with facies association 1 of the planktonic foraminifera domain. The inner parts of the transect are characterised by epiphytic foraminifera (small benthic and large porcelaneous forms) where sea-grass meadows developed in the upper euphotic zone [3] in all studied sections (Fig. 10A).

Basinward of the inner ramp facies, in the Ganaveh and Arand anticlines, the seafloor consisted of large coral build-ups composed of flat and fine-branched coral colonies encrusted by coralline algae (Facies Association 4). The outer platform deposits are represented by thick intervals of shale and marl intercalated with thin limestone beds rich in planktonic foraminifera and LBF fragments (Facies Association 2) towards the Arand and Dehdasht sections. The middle parts of the depositional profile broadly occur in the Ganaveh and Siang sections and are characterized by facies associations 3 and 4.

Aquitanian carbonate ramp

During the Aquitanian, the entire study area occupied the inner to mid parts of the carbonate ramp with a very shallow and low-angle depositional profile based on the dominant lithological characters, relative position of facies belts, biogenic components and stratal architecture (Fig. 10B). The interplay of eustatic sea-level and climate changes at the Chattian-Aquitanian boundary led to the isolation of the Asmari inner shelf from the open sea [1, 3]. Consequently, salinity increased and "basal anhydrite" was deposited in the depocenter of the Asmari intra-shelf at the start of the Aquitanian time [1]. Ooid- and *Favreina*-dominated dolomitic limestones (Facies association 5) along with porcelaneous foraminifera (facies association 4) became the main carbonate factory across the study area during the Aquitanian (Fig. 10B). The very shallow-water carbonate ramp depositional system was generally characterized by ooids and *Favreina* along with low-diversity small benthic foraminifera, representing remnants of the large volumes of sediment that were produced on the inner ramp. For the most part, this Aquitanian carbonate system pinched-out toward the NE as reported by Shabafrooz et al. [3].

Burdigalian carbonate ramp system

During the Burdigalian, a very shallow carbonate ramp (inner ramp) covered the entire study area (Fig. 10C). This carbonate system is represented by larger foraminiferal (Facies association 4) and coralline algal carbonate deposits, representing an inner ramp setting. Biota and texture analysis allow two facies to be distinguished: mud-dominated (FA 6) and small benthic foraminifera facies (FA 4). The proximal inner ramp deposits, show a irregular scattering of numerous dominating biota including LBF, echinoderms, and small benthic foraminifera, bryozoans, corals and coralline algae (in the Arand and Dehdasht sections). Local accumulations of thin shell beds of bivalves and echinoids can be interpreted as representing relatively high-energy nearshore environments with a comparatively high input of terrigenous material. Distal middle ramp deposits are not present. These deposits are present in the western parts of the Dezful embayment oilfields and Izeh Zone outcrops such as the Bangestan anticline [9]. The distal mid to outer ramp setting within the western parts of the Dezful embayment and Izeh Zone are characterized by a regional tilt of the carbonate platform during the Burdigalian. This caused uplift and non-deposition in the SW and a shift of the depocenter toward the NW where subsidence was high and sediment accumulated along a new margin facing the NeoTethys [1, 11, 54-56] (Fig. 10C).

Sequence stratigraphy

Integrating of the facies association, the stacking patterns of the strata and major bound surfaces, along with the environmental dependence of the skeletal components, results in five major depositional sequences (labeled 1-5) being distinguished within the Asmari Fm in the studied area. They are supported by depositional geometry-based correlation enabled by improved foraminifer biostratigraphy (Fig. 11). The main characters and positions of main sequence boundaries are the same as those documented by Van Buchem et al. [1] and Shabafrooz et al. [3]. All five sequences occur at the Ganaveh and Siang sections (Fig. 11), while at the Arand and Dehdasht outcrops, only sequences 3 to 5 are present (Fig. 11). Towards the basin center (Arand and Dehdasht), older sequences (1-3) can be recognized within the Pabdeh Fm. Sequence 1 is Rupelian/Chattian in age, corresponding to the *Nephrolepidina-Operculina-Ditrupea* Assemblage zone (Table 1). The presence of *Archaias* and *Spiroclypeus blankenhorni* confirms that sequences 2 and 3 are Chattian in age. The Aquitanian (depositional sequence 4) and the Burdigalian sequence (depositional sequence 5) correspond to Assemblage 3 and 4, respectively

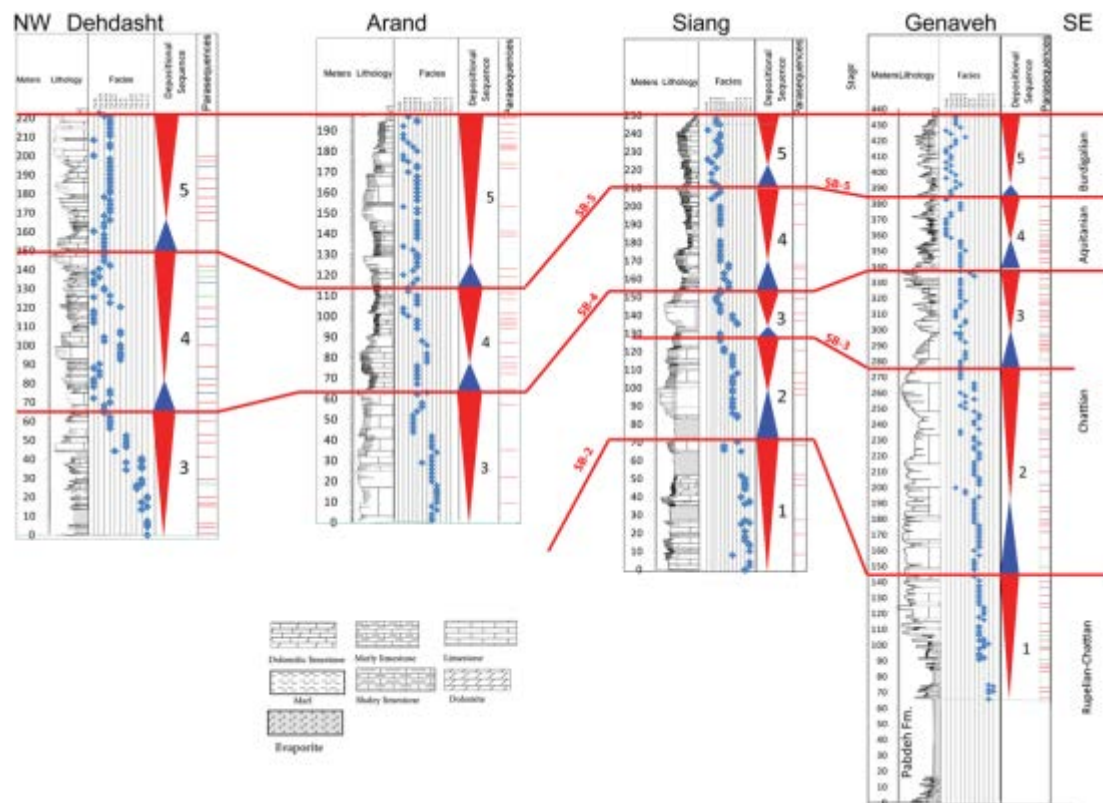


Figure 11. Sequence stratigraphic correlation of the Asmari Fm across the study area

(Table. 1). The identified depositional sequences are described below in ascending order and, where possible, will be compared with the published sequence stratigraphic scheme proposed by Ehrenberg et al. [11], Van Buchem et al. [1] and Shabafrooz et al. [3].

Sequence 1

Sequence 1 present the base of the Asmari Fm at the Ganaveh (78 m; Figs. 3, 11, 12) and Siang (70 m; Figs. 4, 11, 13) outcrops. It overlies the Pabdeh Fm (Fig. 11) and corresponds to sequence C of Shabafrooz et al. [3]. In the Ganaveh and Siang sections, the lower boundary (SB-1) is positioned with uncertainty within the Pabdeh Fm. The transgressive systems tract (TST) consists of an alternation of facies association 1 and facies association 2 representing a transitional zone between the Pabdeh and Asmari formations. The maximum flooding surface (mfs) of this sequence is defined by the landward reworking of the lepidocyclinid-dominated facies towards the Siang and Ganaveh sections. Following the maximum flooding surface (mfs), the regressive phase is marked by a SW-dipping prograding margin which is composed of grain-supported carbonate deposits (Facies association 3 and 4), formed as a result of decreases in accommodation space.

Biostratigraphically, the upper boundary of this sequence (Fig. 13) is significant which is close to the last appearance of *Lepidocyclina* (*Eulepidina dilatata*), with strong bioturbation, especially in the Ganaveh section (Fig. 3 and Table 1). Towards the SW, this boundary could be corresponding to surface Ch20 of Ehrenberg et al. [11] and the truncated surface at the top of the Eshgar and Tang-e-Gurguda clinofolds [3].

Sequence 2

Sequence 2 is characterized by a series of coral build-ups mostly in the Ganaveh (Figs. 3, 8a, 12) and Arand outcrops (Figs. 5, 8b, 11). It is also present in the Siang section without distinctive coral build-ups. This depositional sequence corresponds to the lower part of the sequence D of Shabafrooz et al. [3], which is characterized by several spectacular scattered coral build-ups in the Eshgar and Anneh outcrops. The lower sequence boundary (SB-2) has been described above. The dominant lithology of this depositional sequence includes 46 m of medium- to thick-bedded coral-rich limestones at the Ganaveh section (Fig. 12) and 32 m of thin- to medium-bedded marly limestones at the Siang section (Fig. 13).

The TST of this sequence is defined by a series of

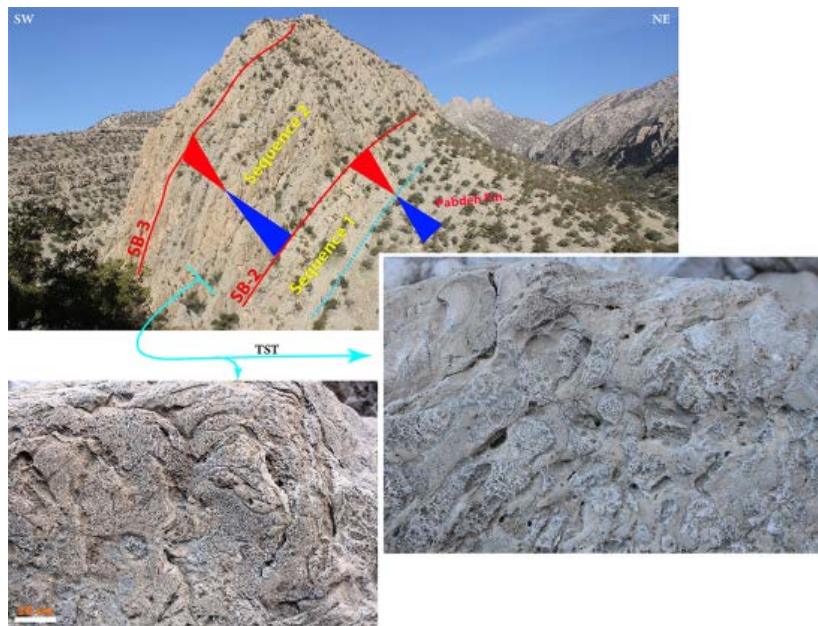


Figure 12. View of the lower part of the Asmari Fm in the Ganaveh section, with interpretation of the depositional sequences. Note significant accumulation of corals in the lower part of Sequence 2.

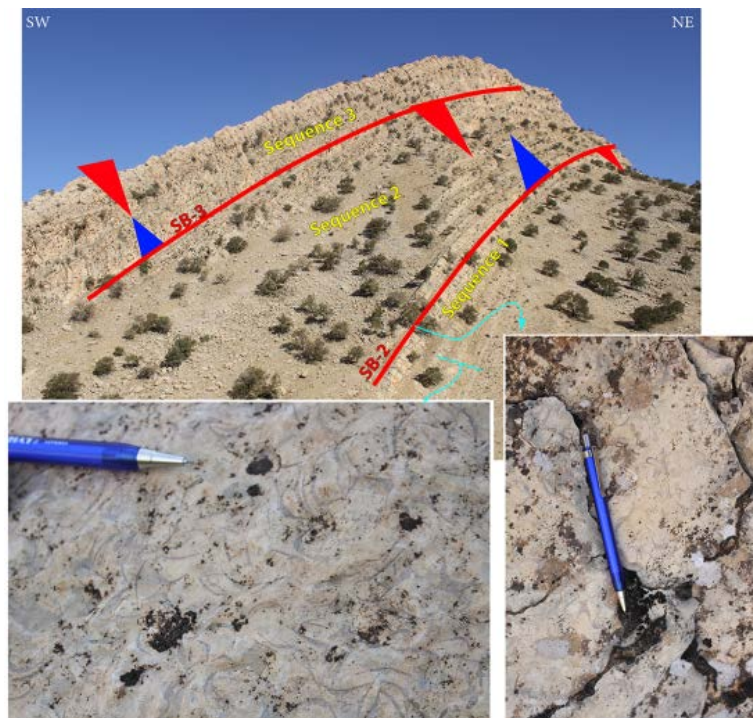


Figure 13. View of the lower part of the Asmari Fm in the Siang section, with interpretation of the depositional sequences. Significant accumulations of *Lepidocylinidae* occur in the lower part of Sequence 1. Note the brecciated layer at the contact between sequences 1 and 2 (SB-2).

deepening-upward parasequences (facies association 3 and 4) with the occurrence of several coral buildups within meter-thick limestone layers (Fig. 12), especially in the Arand and Ganaveh sections. The mfs could be placed on top of the maximum aggradation rate of coral

build-ups. During the highstand systems tract (HST), infilling of the space between the build-ups was initiated. HST is identified by corals and coralline red algae (facies association 3), and perforate and imperforate LBF (facies association 4) that formed

during the sea-level fall. Maximum fall of sea level (SB-3) in the study area is represented by thin beds of brecciated dolomitic limestones in the Siang and Ganaveh sections. In the latter section, there are strongly bioturbated, *Thalassinoides*-rich marly limestone layers close to this surface.

Sequence 3

This depositional sequence consists of medium- to thick-bedded limestones (Fig. 13A) at the Ganaveh (Fig. 3; 56 m) and Siang (Fig. 4; 26 m) sections (Figs. 11, 13). The sequence starts with deposition of the Asmari Fm at the Arand (Fig. 5; 60 m) and Dehdasht (Fig. 6; 65 m) outcrops overlying the basal marl of the Pabdeh Fm (Fig. 11). The TST of the sequence occurs at the Ganaveh and Siang sections and is composed of benthic foraminifera-rich facies (facies association 2: mainly *Neorotalia* and *Miogypsinoides*) forming several deepening-upward cycles.

The maximum flooding sediments are characterized by an interval of marly limestones, dominated by hyaline LBF (mainly *Spirochlypeus*) followed by shallowing-upward cycles. The latter mostly represent carbonate sediments of the HST with proximal inner ramp facies (facies association 4; Fig. 11) displaying a shallowing-upward trend. The upper boundary of this sequence (SB-4) is defined on top of a shallow-water carbonate. In the Siang section, this is locally overlain

by a thin brecciated layer (Fig. 14). This surface is also a significant biostratigraphic event, belong to the last appearance of *Archaias* (*A. kirkukensis* and *A. hensoni*), corresponds to the “*Archaias asmaricus*- *A. hensoni*-*Miogypsinoides complanatus*” Assemblage Zone (Assemblage C; Table 1) of Van Buchem et al. [1], close to the Oligocene-Miocene boundary (Chattian–Aquitania). This surface is equivalent to the surface Aq-10 documented by Ehrenberg et al. [11], surface IV of Van Buchem et al. [1] and SB-E of Shabafrooz et al. [2 and 3].

Sequence 4

The Sequence 4 (Aquitania) is well-exposed in the Ganaveh (45 m), Siang (56 m; Fig. 14), Arand (53 m; Fig 15) and Dehdasht (84 m; Fig. 16) sections. During the rise of sea level (TST), deposition took place in shallow subtidal and aggradational stacking patterns formed within study area (Fig. 11). These deposits are composed of dolomitized limestones as well as miliolid- and ooid/*Favreina*-dominated shoal deposits. The mfs is placed within the wackestone–packstone with a diverse fauna including small rovaliids, discorbids, bryozoans, and echinoid spines, which is one of the deepest facies of the Aquitania. This is followed by a shallowing-upward trend of the restricted lagoonal deposits of the inner ramp and is interpreted to be HST carbonates rich in imperforate foraminifera.

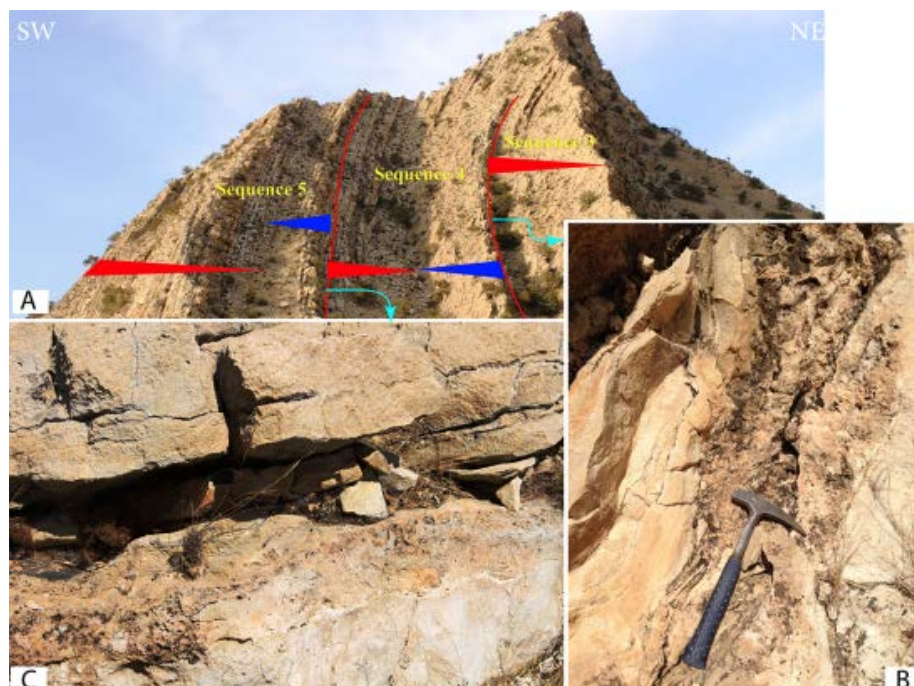


Figure 14. Aspects of key outcrops of the Asmari Fm in the Siang section. A) Upper part of the Asmari Fm, with interpretation of the depositional sequences. B) Thin layer of red-stained breccia at the contact of depositional sequences 3 and 4 (SB-4). C) Brecciated surface with extensive dissolution features at the contact of depositional sequences 4 and 5 (SB-5).

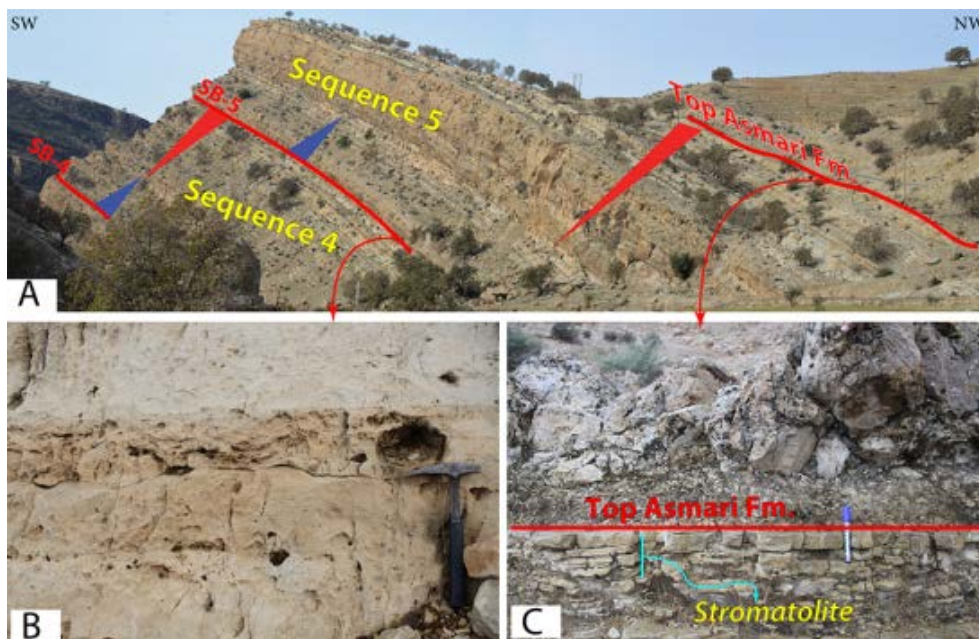


Figure 15. Characteristic features of key outcrops of the Asmari Fm in the Arand section. A) View of the upper part of the Asmari Fm in the Arand section, with interpretation of the depositional sequences. B) Thin layer of red-stained breccia at the contact of depositional sequences 4 and 5 (SB-5). C) Stromatolite layer with thin lamination at the contact between the Asmari and Gachsaran formations (SB-6).

The upper boundary (SB-5) of this sequence is represented by a bed of red breccia, with iron hydroxides and shell fragments (bivalves, bryozoans) (Figs. 14C, 15B, 16C). This surface marks the boundary between the Aquitanian and Burdigalian, and is well constrained by both the occurrence of the benthic index fossil *Borelis melo curdica* in the Burdigalian and the Sr isotope dating documented by Ehrenberg et al. [11] and Van Buchem et al. [1] in the Dezful Embayment. This sequence boundary is also comparable with the surface Bu10 documented by Ehrenberg et al. [11], surfaces V+VI of Van Buchem et al. [1] and SB-F of Shabafrooz et al. [3].

Sequence 5

This depositional sequence is Burdigalian in age and can be correlated with sequence F of Shabafrooz et al. [3]. It is present in the Ganaveh (53 m), Siang (40 m; Fig. 14), Arand (87 m; Fig 15) and Dehdasht (72 m; Fig; 16) sections. The lower boundary (SB-5) has been described above. The TST sediments of this sequence are characterized by very shallow facies rich in porcelaneous foraminifera together with corals and corallinean debris (facies association 4). The sediments of mfs are rich in small rotaliids and small benthic foraminifera along with echinoderm remains. The HST is characterized by porcelaneous foraminifera together with corals and corallinean debris and

terminates with abundant porcelaneous benthic foraminifera. During the HST, very diverse porcellaneous forms abounded in the basin, followed by carbonate mud-dominated facies. The upper boundary (SB-6) of this sequence is placed at the base of Gachsaran Formation, represented by a very thin stromatolitic layer in the Arand (Fig. 15C) and Dehdasht sections.

Discussion

Relative sea-level changes and depositional settings

On the bases of depositional geometries, lithostratigraphy, biostratigraphy, biogenic contents and lateral and vertical variations of facies the stratigraphic model of the Asmari Fm schematically summarized in Figure 17, appears as a large systematic progradation (from SE/E to NW/W) over the basinal Pabdeh Fm during Oligo-Miocene times. The overall thickness of the Asmari Fm decreases from SE (Ganaveh) to NW (Dehdasht). The lower boundary of the Asmari Fm is younging towards the basin center, from SE and E to NW and W (Figs. 11 and 17). The Chattian time interval is characterized by installation of corals/coralalgal bodies (Facies association 3; Table 2 and Fig. 17) over the Pabdeh Fm with a downward shift of facies, toward the basin (NW; Arand section). This deposits consists of coarse-grained bioclast floatstone that dominated by

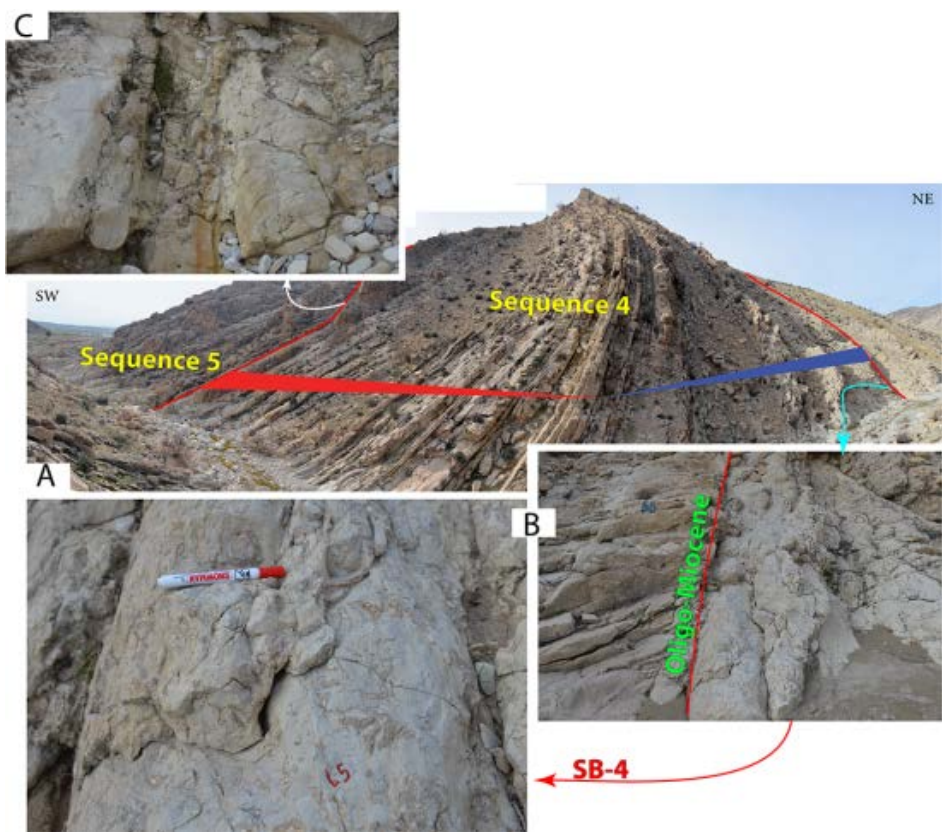


Figure 16. Photograph of the Asmari Fm at the Dehdasht section. A) General view with interpretation of the depositional sequences. B) Distant and close-up view of a brecciated and shell-rich layer (SB-4) between depositional sequences 3 and 4. C) Thin layer of red-stained breccia at the contact of depositional sequences 4 and 5 (SB-5).

tabular to domical coral and coralline red and benthic foraminifera packstone/grainstone (Facies association 4; Table 2) mainly in the southeastern part (Ganaveh and Siang sections) of the transect.

Sea-level fluctuations in the studied interval were interpreted using regional geometrical reconstructions, sedimentological facies associations and high-resolution time-lines. Although, the sequence subdivision

proposed here for the Oligo-Miocene time interval and those reported by Ehrenberg et al. [11], Van Buchem et al. [1] and Shabafrooz et al. [3] (Fig. 18).

Development of the Rupelian/Chattian carbonate ramp (including sequence 1) in the Ganaveh and Siang area could be connected to Chattian sea-level falls [57, 58]. The scale of sea-level fluctuation varied during the early Chattian corresponding to the formation of a series

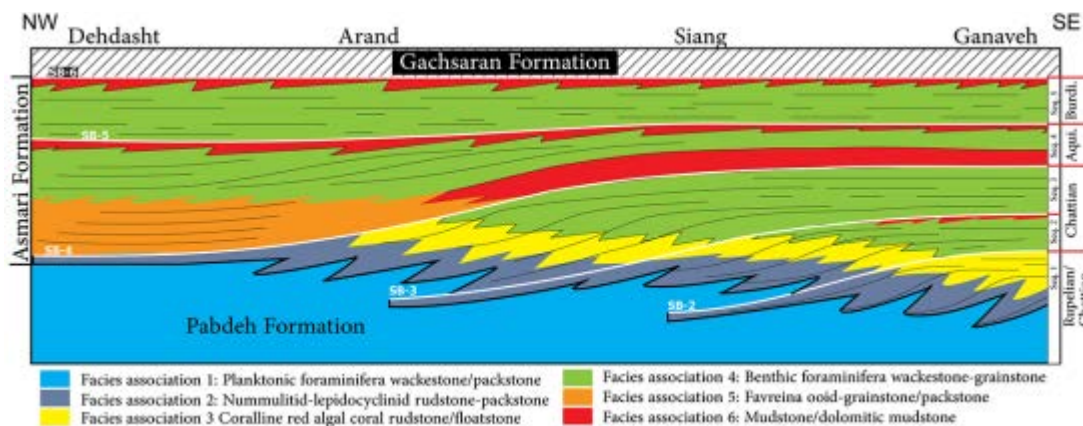


Figure 17. Stratigraphic model of the Asmari Fm based on the correlation of the 4 studied sections

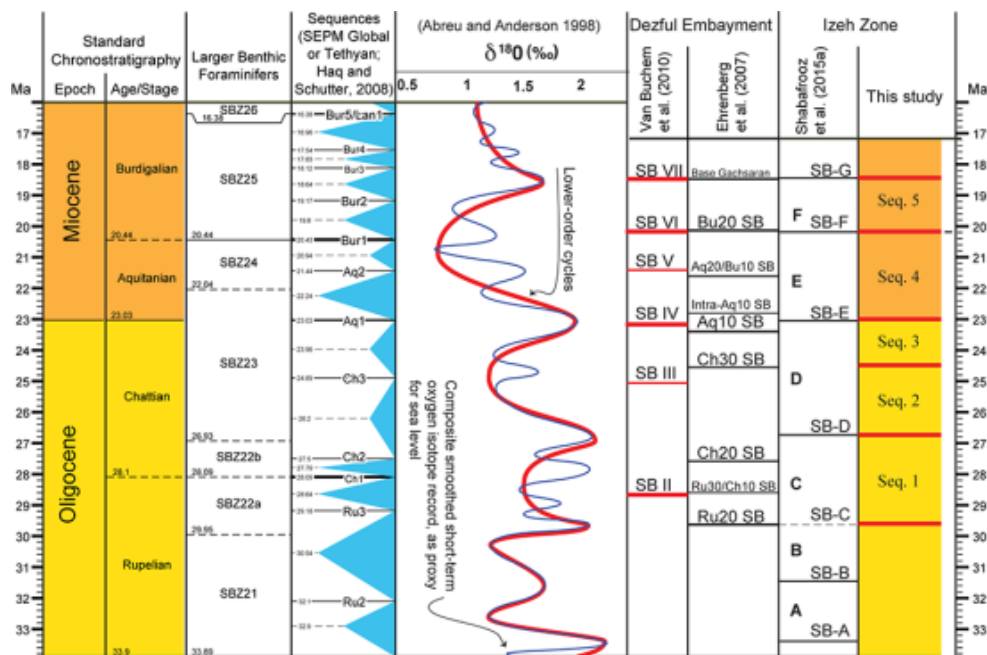


Figure 18. Comparison of the proposed depositional sequences with those recognized in neighboring areas and with the global sea-level curve.

of coral- algal-dominated carbonate deposits (including sequences 2 and 3), as is clearly showed by a suite of buildups in the Arand and Ganaveh outcrops.

The Aquitanian deposits are very shallow and composed of very proximal inner ramp facies (Facies association 5 and 6; Fig. 17 and Table 2) through the field from SE-NW. The Early Miocene time is the final stage of long-lived progradational carbonate platform system of the Asmari Fm (sequences 4 and 5) that filled the intra-shelf seaway [1, 3]. This is characterized by the association of ooid- and *Favreina*-dominated facies (Facies association 5; Table 2). Furthermore, glacio-eustatic sea-level oscillations [58] and arid semi-arid climatic conditions ruled the numerous phases of desiccation and evaporate deposition in the basins (e.g., Van Buchem et al. [1]).

The subsequent rise of sea-level led to development of a low-angle dolomitic carbonate ramp with abundant LBF (Sequence 5) that is well-exposed in the study area. This event can be recognized on the average oxygen stable isotope curve of Abreu and Anderson [59] (Fig. 18). The Burdigalian strata are also very flat and composed of highly dolomitized very proximal inner ramp facies (Facies associations 4 and 6). These series are then capped by evaporate-dominated Gachsaran Formation (Fig. 17).

Conclusions

Index fossils identified in the study area show that

the Asmari Fm has been deposited during the Rupelian-Chatthian to Early Miocene times. The Asmari Fm shows a diachronous stratigraphic boundary with the underlying Pabdeh Fm which was dated stepwise to the Rupelian/Chatthian in the Ganaveh section (SE) and subsequently became younger (Chatthian) toward the Dehdasht section (NW).

Six facies associations (FA.1-6) were identified with the semi-quantitative analysis of both microscopic and macroscopic observations—e.g., texture, skeletal components and size and shape of grains. The vertical distribution of facies showed that the Asmari Fm was formed as a carbonate ramp dominated by large benthic foraminifera, coralline red algae and corals during the Rupelian-Chatthian/Chatthian. This biota lived in the outer, middle and inner ramp. During the Early Miocene time, non-skeletal components (ooids and *Favreina*) along with porcelaneous foraminifera occurred only in the middle and inner low-angle ramp. Based on the stratal stacking patterns and facies interpretations, five 3rd-order depositional sequences were identified, representing a systematic progradations from SE to NW into and over the basinal Pabdeh Fm. These depositional sequences can be correlated from the Ganaveh to the Dehdasht sections and document significant changes in the facies and evolution of the Asmari platform during the Oligo-Miocene time interval.

References

1. Van Buchem F.S.P., Allan T.L., Laursen G.V., Lotfpour M., Moallemi A., Monibi S., Motiei H., Pickard N.A.H., Tahmasbi A.R., Vedrenne V., and Vincent B. Regional stratigraphic architecture and reservoir types of the Oligo-Miocene deposits in the Dezful Embayment (Asmari and Pabdeh Formations) SW Iran. *Geological Society, London, Special Publications*. **329**(1): 219–263 (2010).
2. Shabafrooz R., Mahboubi A., Vaziri-Moghaddam H., Moussavi-Harami R., Ghabeishavi A., and Al-Aasm I.S. Facies analysis and carbonate ramp evolution of Oligo-Miocene Asmari Formation in the Gachsaran and Bibi-Hakimeh oilfields and the nearby Mish anticline, Zagros Basin, Iran *Neues Jahrbuch für Geologie und Paläontologie - Abhandlungen*. **276**(1): 121-146 (2015).
3. Shabafrooz R., Mahboubi A., Vaziri-Moghaddam H., Ghabeishavi A., and Moussavi-Harami R. Depositional architecture and sequence stratigraphy of the Oligo-Miocene Asmari platform; Southeastern Izeh Zone, Zagros Basin, Iran. *Facies*. **61**(1): 1-32 (2015).
4. Thomas A.N. The Asmari Limestone of south-west Iran. In: Hobson, G.D. (Ed.), International Geological 124 Strontium isotope stratigraphy, Asmari Formation SW Iran Congress, report of 18th session Great Britain 1948, part IV, proceedings of section E, the geology of petroleum. *IGC Publication, London*: 35-44 (1950).
5. James G.A. and Wynd J.G. Stratigraphic nomenclature of Iranian Oil Consortium Agreement Area. *AAPG Bulletin*. **49**(12): 2182–2245 (1965).
6. Adams T.D. The Asmari Formation of Lurestan and Khuzestan provinces. Iranian Oil Operating Companies, Geological and Exploration Division, Report, no. 1154.: (1969).
7. Adams C. and Bourgeois E., Asmari biostratigraphy. *Geological and Exploration Div. Iranian Oil Offshore Company. Unpublished Report 1074*. (1967).
8. Vaziri-Moghaddam H., Seyrafian A., Taheri A., and Motiei H. Oligo-Miocene ramp system (Asmari Formation) in the NW of the Zagros basin, Iran: Microfacies, paleoenvironment and depositional sequence. *Revista Mexicana de Ciencias Geológicas*. **27**(1): 56–71 (2010).
9. Rahmani A., Taheri A., Vaziri-Moghaddam H., and Ghabeishavi A. Biostratigraphy of the Asmari Formation at Khaviz and Bangestan Anticlines, Zagros Basin, SW Iran. *Neues Jahrbuch für Geologie und Paläontologie-Abhandlungen*. **263**(1): 1–16 (2012).
10. Allahkarampour Dill M., Seyrafian A., and Vaziri-Moghaddam H. Palaeoecology of the Oligocene-Miocene Asmari Formation in the Dill Anticline (Zagros Basin, Iran). *Neues Jahrbuch für Geologie und Paläontologie - Abhandlungen*. **263**(2): 167-184 (2012).
11. Ehrenberg S.N., Pickard N.A.H., Laursen G.V., Monibi S., Mossadegh Z.K., Svånå T.A., Aqrabi A.A.M., McArthur J.M., and Thirlwall M.F. Strontium isotope stratigraphy of the Asmari Formation (Oligocene - lower Miocene), SW Iran. *Journal of Petroleum Geology*. **30**(2): 107–128 (2007).
12. Rahmani A., Vaziri-Moghaddam H., Taheri A., and Ghabeishavi A. A model for the paleoenvironmental distribution of larger foraminifera of Oligocene–Miocene carbonate rocks at Khaviz Anticline, Zagros Basin, SW Iran. *Historical Biology: An International Journal of Paleobiology*. **21**(3): 215–227 (2009).
13. Vaziri-Moghaddam H., Kimiagari M., and Taheri A. Depositional environment and sequence stratigraphy of the Oligo-Miocene Asmari Formation in SW Iran. *Facies*. **52**(1): 41–51 (2006).
14. Sadeghi R., Vaziri-Moghaddam H., and Taheri A. Microfacies and sedimentary environment of the Oligocene sequence (Asmari Formation) in Fars sub-basin, Zagros Mountains, southwest Iran. *Facies*. **57**(3): 431-446 (2011).
15. Seyrafian A. Microfacies and depositional environments of the Asmari Formation, at Dehdez Area (a correlation across central Zagros Basin). *Carbonates and Evaporites*. **15**(2): 121–129 (2000).
16. Allahkarampour Dill M., Seyrafian A., and Vaziri-Moghaddam H. The Asmari Formation, north of the Gachsaran (Dill anticline), southwest Iran: facies analysis, depositional environments and sequence stratigraphy. *Carbonates and Evaporites*. **25**(2): 145–160 (2010).
17. Alavi M. Structures of the Zagros fold-thrust belt in Iran. *American Journal of Science*. **307**(9): 1064-1095 (2007).
18. Sepehr M. and Cosgrove J.W. Structural framework of the Zagros Fold-Thrust Belt, Iran. *Marine and Petroleum Geology*. **21**(7): 829-843 (2004).
19. Falcon N. Southern Iran: Zagros Mountains. *Geological Society London Special Publications*. **4**(1): 199 (1974).
20. Berberian M. Master "blind" thrust faults hidden under the Zagros folds: active basement tectonics and surface morphotectonics. *Tectonophysics*. **241** 193-224 (1995).
21. Embry A. and Klovan J. A late Devonian reef tract on northeastern Banks Island, NWT. *Bulletin of Canadian Petroleum Geology*. **19**(4): 730 (1971).
22. Flügel E., Microfacies of Carbonate Rocks, Analysis, Interpretation and Application. 2010, Berlin, 976 P: Springer-Verlag. 976.
23. Dunham R. Classification of carbonate rocks according to depositional texture, in Classification of Carbonate Rocks—a symposium, *AAPG Mem*, H. WE, Editor. 1962. p. 108–121.
24. Adams C. and Bourgeois E. Asmari biostratigraphy. *Geological and Exploration Div. Iranian Oil Offshore Company. Report 1074*. 1967, Unpublished.
25. Wynd J.G. Biofacies of the Iranian consortium-agreement area, *Unpublished Report 1082*. 1965, Iranian Offshore Oil Company: Tehran.
26. Cahuzac B. and Pognant A. An attempt of biozonation of the Oligo-Miocene in the European basins by means of larger neritic foraminifera. *Bulletin- Societe Geologique De France*. **168**(2): 155-170 (1997).
27. Gatt P.A. and Gluyas J.G. Climatic controls on facies in Palaeogene Mediterranean subtropical carbonate platforms. *Petroleum Geoscience*. **18**(3): 355–367 (2012).
28. Buxton M.W.N. and Pedley H.M. A standardized model for Tethyan Tertiary carbonate ramps. *Journal of the Geological Society*. **146**: 746–748 (1989).
29. Cosovic V., Drobne K., and Moro A. Paleoenvironmental model for Eocene foraminiferal limestones of the Adriatic carbonate platform (Istrian Peninsula). *Facies*. **50**: 61–75 (2004).

30. Corda L. and Brandano M. Aphotic zone carbonate production on a Miocene ramp, Central Apennines, Italy. *Sedimentary Geology*. **161**(1-2): 55–70 (2003).
31. Romero J., Caus E., and Rosell J. A model for the palaeoenvironmental distribution of larger foraminifera based on late Middle Eocene deposits on the margin of the South Pyrenean basin (NE Spain). *Palaeogeography, Palaeoclimatology, Palaeoecology*. **179**(1-2): 43–56 (2002).
32. Geel T. Recognition of stratigraphic sequences in carbonate platform and slope deposits: empirical models based on microfacies analysis of Palaeogene deposits in southeastern Spain. *Palaeogeography, Palaeoclimatology, Palaeoecology*. **155**: 211–238 (2000).
33. Pomar L., Mateu-Vicens G., Morsilli M., and Brandano M. Carbonate ramp evolution during the Late Oligocene (Chattian), Salento Peninsula, southern Italy. *Palaeogeography, Palaeoclimatology, Palaeoecology*. **404**(1): 109–132 (2014).
34. Brandano M., Lipparini L., Campagnoni V., and Tomassetti L. Downslope-migrating large dunes in the Chattian carbonate ramp of the Majella Mountains (Central Apennines, Italy). *Sedimentary Geology*. **256**: 29–41 (2012).
35. Pomar L., Bassant P., Brandano M., Ruchonnet C., and Janson X. Impact of carbonate producing biota on platform architecture: Insights from Miocene examples of the Mediterranean region. *Earth-Science Reviews*. **113**(3–4): 186–211 (2012).
36. Hohenegger J. Estimation of environmental paleogradient values based on presence/absence data: a case study using benthic foraminifera for paleodepth estimation. *Palaeogeography Palaeoclimatology Palaeoecology*. **217**(1-2): 115–130 (2005).
37. Brandano M., Frezza V., Tomassetti L., Pedley M., and Matteucci R. Facies analysis and palaeoenvironmental interpretation of the Late Oligocene Attard Member (Lower Coralline Limestone Formation), Malta. *Sedimentology*. **56**(4): 1138–1158 (2009).
38. Brandano M., Frezza V., Tomassetti L., and Cuffaro M. Heterozoan carbonates in oligotrophic tropical waters: The Attard member of the lower coralline limestone formation (Upper Oligocene, Malta). *Palaeogeography, Palaeoclimatology, Palaeoecology*. **274**(1-2): 54–63 (2009).
39. Brandano M., Morsilli M., Vannucci G., Parente M., Bosellini F., and Mateu-Vicens G. Rhodolith-rich lithofacies of the Porto Badisco Calcarenes (upper Chattian, Salento, southern Italy). *Italian Journal of Geosciences*. **129**(1): 119–131 (2010).
40. Morsilli M., Bosellini F.R., Pomar L., Hallock P., Aurell M., and Papazzoni C.A. Mesophotic coral buildups in a prodelta setting (Late Eocene, southern Pyrenees, Spain): a mixed carbonate–siliciclastic system. *Sedimentology*. **59**(3): 766–794 (2012).
41. Nebelsick J.H., Stingl V., and Rasser M. Autochthonous facies and allochthonous debris flows compared: Early Oligocene carbonate facies patterns of the Lower Inn Valley (Tyrol, Austria). *Facies*. **44**: 31–46 (2001).
42. Barbieri M., Castorina F., Civitelli G., Corda L., Madonna S., Mariotti G., and Milli S. Carbonate ramp sedimentation of the Prenestini Mountains (Lower Miocene, Central Apennines): Sedimentation, sequence stratigraphy and strontium isotope stratigraphy. *Geologica Romana*(37): 79–96 (2003).
43. Frezza V., Mateu-Vicens G., Gaglianone G., Baldassarre A., and Brandano M. Mixed carbonate-siliclastic sediments and benthic foraminiferal assemblages from *Posidonia oceanica* seagrass meadows of the central Tyrrhenian continental shelf (Latium, Italy). *Italian Journal of Geosciences*. **130**(3): 352–369 (2011).
44. Mateu-Vicens G., Box A., Deudero S., and Rodríguez B. Comparative analysis of epiphytic foraminifera in sediments colonized by seagrass *Posidonia oceanica* and invasive macroalgae *Caulerpa* spp. *The Journal of Foraminiferal Research*. **40**(2): 134–147 (2010).
45. Pomar L. and Kendall C.G.S.C. Architecture of carbonate platforms; a response to hydrodynamics and evolving ecology, in Controls on Carbonate Platform and Reef Development, J. Lukasik & A. Simo (Eds.). *SEPM Special Publication*(89): 187–216 (2008).
46. Pomar L., Brandano M., and Westphal H. Environmental factors influencing skeletal grain sediment associations: a critical review of Miocene examples from the western Mediterranean. *Sedimentology*. **51**(3): 627–651 (2004).
47. Brasier M.D. An outline history of seagrass communities. *Palaeontology* **18**(4): 681–702 (1975).
48. Langer M.R. Epiphytic foraminifera. *Marine Micropaleontology*. **20**(3–4): 235–265 (1993).
49. Wenk H.-R., Barber D.J., and Reeder R.J. Microstructures in carbonates. *Reviews in Mineralogy and Geochemistry*. **11**(1): 301–367 (1983).
50. Mateu-Vicens G., Hallock P., and Brandano M. A Depositional Model and Paleocological Reconstruction of the Lower Tortonian Distally Steepened Ramp of Menorca (Balearic Islands, Spain). *Palaaios*. **23**(7): 465–481 (2008).
51. Carpentier C., Lathuilière B., Ferry S., and Sausse J. Sequence stratigraphy and tectosedimentary history of the Upper Jurassic of the Eastern Paris Basin (Lower and Middle Oxfordian, Northeastern France). *Sedimentary Geology*. **197**(3-4): 235–266 (2007).
52. Bádenas B. and Aurell M. Facies models of a shallow-water carbonate ramp based on distribution of non-skeletal grains (Kimmeridgian, Spain). *Facies*. **56**(1): 89–110 (2010).
53. Pomar L. Types of carbonate platforms: a genetic approach. *Basin Research*. **13**: 313–334 (2001).
54. Sampo M., ed. Microfacies and Microfossils of the Zagros Area Southwestern Iran (From Pre Permian to Miocene). *International Sedimentary Petrographical Series*. E. J. Brill, Leiden, 1–102, ed. J. Cuvillier and H.M.E. Schurmann. **Vol. 12**. 1–102 (1969).
55. Thomas A.N. Facies variations in the Asmari Limestone. In: Thomas, H.D. (Ed.) International Geological Congress report of the 18th session Great Britain 1948, part X, Proceedings of section J, faunal and floral facies and zonal correlation. *International Growth Centre (IGC Publication), London*: 74–82 (1952).
56. Thomas A.N. The Asmari Limestone of south-west Iran. In: Hobson, G.D. (Ed.), International Geological 124 Strontium isotope stratigraphy, Asmari Formation SW

- Iran Congress, report of 18th session Great Britain 1948, part IV, proceedings of section E, the geology of petroleum. *IGC Publication, London*: 35–44 (1948).
57. Miller K.G., Wright J.D., and Fairbanks R.G. Unlocking the Ice House: Oligocene-Miocene oxygen isotopes, eustasy, and margin erosion. *Journal of Geophysical Research: Solid Earth*. **96**(B4): 6829-6848 (1991).
58. Abreu V.S. and Haddad G.A. Glacioeustatic variations: the mechanism linking stable isotope events and sequence stratigraphy from the early Oligocene to Middle Miocene. *SEPM Special Publication*. **60**: 245–260 (1998).
59. Abreu V.S. and Anderson J.B. Glacial eustasy during the Cenozoic; sequence stratigraphic implications. *AAPG Bulletin*. **82**(7): 1385-1400 (1998).